Sensors and Actuators A 318 (2021) 112486

Contents lists available at ScienceDirect

Sensors and Actuators A: Physical

journal homepage: www.elsevier.com/locate/sna

Porous silicon membranes and their applications: Recent advances

Roselien Vercauteren[a,*], Gilles Scheen[b], Jean-Pierre Raskin[a], Laurent A. Francis[a]

[a] UCLouvain, ICTEAM Institute, Electrical Engineering Dpt., Place du Levant 3, B - 1348 Louvain-la-Neuve, Belgium
[b] Incize, Chemin du Cyclotron 6, B-1348 Ottignies-Louvain-la-Neuve, Belgium

ARTICLE INFO

Article history:
Received 5 October 2020
Received in revised form
20 November 2020
Accepted 2 December 2020
Available online 4 December 2020

Keywords:
Porous silicon
Membrane fabrication
Tissue engineering scaffold
Biosensor
Microfuel cell

ABSTRACT

Porous silicon (PSi) research has been active for several decades. The multiple properties and structural features of PSi have made it a promising material for a wide variety of applications, going from drug delivery to microelectronics. By removing the bulk silicon below a PSi layer and creating a membrane, a whole new set of physical and chemical characteristics as well as potential uses have been discovered. In this review, recent works on Porous silicon membranes (PSiMs) are analysed and summarised. An updated overview of the progress made in several areas is presented with the purpose of highlighting PSiM's potential. New methods for the fabrication and the integration of PSiMs have been developed, relying more and more on semiconductors microfabrication techniques. Likewise, the properties of PSiMs have been extensively studied, enabling the emergence of a multitude of PSiM-based systems. A critical analysis of the advantages and disadvantages of this material is made, with the emphasis on the integration challenges that PSiMs are facing for future industrialisation.

Contents

* Corresponding author.
E-mail addresses: roselien.vercauteren@uclouvain.be (R. Vercauteren), laurent.francis@uclouvain.be (L.A. Francis).

https://doi.org/10.1016/j.sna.2020.112486
0924-4247/

1. Introduction

Silicon (Si) technology has dominated microelectronics for more than half a century. Not only is silicon the second most abundant material on earth, but it is also characterised by properties that ideally balance performance and stability [1]. In recent decades, microelectronics has permeated to other areas of applications: it is no longer limited to digital circuits but is included in so-called More-than-Moore devices. These devices are used, among others, for sensing, optics, radio frequency (RF), microelectromechanical systems (MEMS) or power electronics. To enable this diversification of applications, the functionality of silicon technology was increased, and the porosification of silicon presented a simple and cheap way to allow its expanded use. Porous silicon (PSi) indeed exhibits properties that are remarkably different from bulk silicon and which can be fine-tuned by adapting the porous morphology. To fabricate PSi, conventional techniques such as lithography and dry etching can be used. Other approaches however exist, a well established one being the use of electrochemical etching.

PSi was first discovered in the mid 1950s by Arthur Jr. and Ingeborg Ulhir [2]. The Uhlirs were initially studying new techniques for polishing silicon surfaces when they accidentally fabricated the first porous silicon film. Their discovery was however more or less forgotten until the late 1980s and early 1990s, when PSi was found to exhibit properties of quantum confinement [3,4]. This breakthrough spurred the scientific communities' interest in PSi and its many properties. Among the topics that emerged back then was the fabrication of porosified silicon membranes [5,6]. Membranes can be defined as interfaces, separating two phases and restricting the transport between those two phases. Porous silicon membranes (PSiMs) are therefore permeable barriers, formed by detaching a porous layer from the underlying bulk silicon substrate. Pores become open-ended channels, enabling a flow-through applications. Obvious applications for PSiMs therefore include separation, adsorption or transport of molecules, ions or small particles. PSiMs are also important tools for the characterisation of PSi, as its properties can be studied in isolation, without the subjacent silicon substrate. The flexibility of the porosification process enables the fabrication of PSiMs with a wide variety of structural features: PSiMs can be ultra-thin or up to 1 mm thick; they can be qualified as micro-, meso- or macroporous depending on the pore size; and their porosity can vary at will within a single membrane.

The interest in PSiMs steadily grew over the years as they can be utilised for their chemical, optical, thermal and structural properties. For instance, PSiMs are used in biomedical applications because of their biocompatibility [7–18]. Their large surface area and open-ended geometry, allowing flow-through operation, makes them ideal for sensing applications [19–23]. Their distinct thermal, electrical and optical properties also make them suitable for microelectronics devices, including thermal insulators [24–26] and micro fuel cells [27–37].

This review concentrates on porous silicon membranes and their integration into various devices. While other PSi nanomaterials, such as PSi nanowires and PSi nanoparticles, have been covered by numerous studies over the last years [38–44], these topics will not be discussed here as they have lately been the subjects of separate reviews [45–47]. The present review only focuses on recent advances from 2014 onward in the field of PSiMs, since the 2014-edition of the *Handbook of Porous Silicon* [48] dedicates an entire chapter to this matter. This review addresses new works in terms of the fabrication, the properties and the applications of PSiMs. Section 2 provides a quick reminder of the fundamentals of electrochemical etching. Section 3 describes the different membranes types and their manufacturing process. Section 4 details their properties, including thermal, mechanical, electrical and optical features. Section 5 discusses several applications in modern fields of science such as biomedical, sensing and energy conversion. Finally, the integration challenges of PSiMs in industrial devices with are briefly discussed in Section 6, before the general conclusions.

2. The fundamentals of PSi

The global interest of the scientific community in porous silicon can be explained by its wide range of features. The multiple fabrication processes enable the creation of porous silicon with various structural attributes. Pore size for example, can vary from a few nanometers to tens of microns. Likewise, the film thickness can be expressed both in nanometers or in microns. Other parameters, like porosity, pore distribution and pore shape can also be controlled by the fabrication process.

Several approaches are therefore used to fabricate porous silicon, mainly relying on dry etching or on electrochemistry. The dry etching technique requires the use of a hard mask to define the holes that will be anisotropically formed by plasma etching. For the electrochemical approach, two principal methods can be distinguished: electrochemical etching and stain etching. The latter relies on the spontaneous electroless etching of silicon when placed in a oxidising hydrofluoric acid (HF)-containing solution [48]. When combined with metal films or nanoparticles, this technique becomes Metal-Assisted Chemical Etching (MACE) [49]. As to date no recent works concerning MACE-fabricated PSiMs have been found by the authors, this review will not include this fabrication technique and mainly focus on electrochemical and dry etching.

Electrochemical etching, which is also called the anodisation method, relies on the wet etching of monocrystalline silicon under the application of an electric current, using an electrolyte containing HF [50]. The current method can be carried out in either a double bath etching cell, with two platinum electrodes, or in a single bath etching cell where the silicon wafer serves as anode and a platinum wire acts as cathode. The etching cells are fabricated in HF-resistant materials, like Teflon® or polyether ether ketone (PEEK). A schematic illustration of a single etching cell is represented in Fig. 1,(a).

Two regimes can be observed within the electrochemical process: pore formation and electropolishing. The transition between those two regimes depends on the substrate's properties, like doping or crystalline orientation, and the fabrication parameters, such as electrolyte concentration and temperature, but is mostly governed by the ratio between the applied current density and the concentration of fluorine ions, as depicted in Fig. 1,(b). The formation of pores in silicon is controlled by energy bonds. By applying a current, electron holes reach the surface and weaken the Si-H bonds. These bonds can then be substituted by Si-F bonds, which

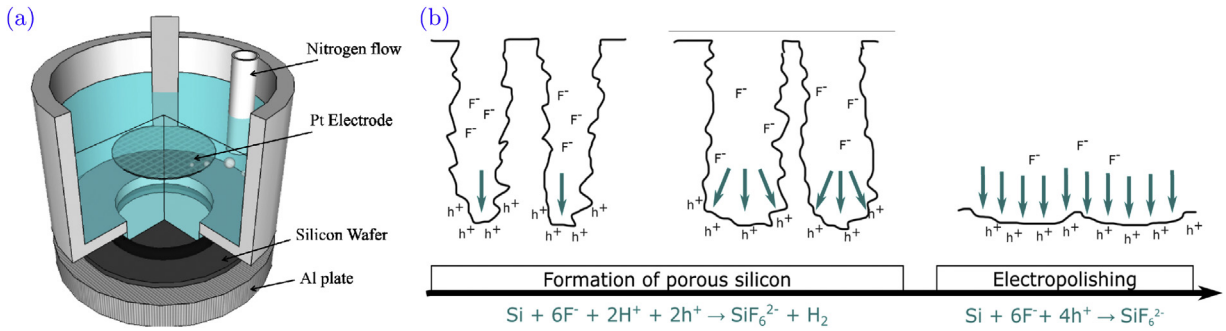

Fig. 1. (a) Illustration of an electrochemical etching cell; (b) Mechanism of pore formation with increasing current densities. The holes reaching the pore tips weaken the Si-H surface bonds and allow the dissolution of the silicon. By increasing the current density, the pore walls become thinner, until the pores merge in the electropolishing regime. Reprinted with permission from [51].

are strongly polarised. Si-Si bonds are then weakened and attacked, resulting in the release of SiF_4 molecules and the creation of a gap in the silicon surface. After pore nucleation, current flows preferentially at the tip of the pore. A space-charge region is also created at the pore walls, preventing lateral etching. By increasing the current density, this space charge region decreases. When the pores start to merge, the electropolishing regime is reached.

PSi is often classified based on the pore size: microporous PSi has an average pore diameter inferior to 2 nm; mesoporous PSi is characterised by a pore size ranging from 2 to 50 nm; and macroporous PSi has a pore size larger than 50 nm. As pore size depends on the doping of the silicon substrate and on the fabrication parameters, it can often be fine-tuned by selecting the appropriate current density and electrolyte composition. The morphology of the pores is also affected by these anodisation parameters, as well as by the doping and the crystal orientation of the silicon substrate: pores can be straight or branched, cylindrical or pyramidal. Porosity is another important parameter, defining the ratio of empty volume to the total volume of the porous region. It is also linked to the substrate doping and the etching parameters. Predicting the pore size, thickness and porosity of a PSi sample with accuracy remains challenging, especially since most of the fabrication parameters are not independent. For example, by increasing the current density used to fabricate mesoporous PSi, not only is the pore diameter increased, but so is the porosity and the thickness of the porous layer. Varying the current density during a single electrochemical etch has been reported for the formation of multi-layers, which resulted in the creation of Bragg filters or optical microcavities [52]. The flexibility of electrochemical etching therefore enables the creation of complex porous structures with calibrated structural properties.

More theoretical details about electrochemical etching are provided in several sources [53,54,48,50]. For a practical guide to anodisation, *Sailor*'s *Porous Silicon in Practice* [52] offers both theoretical details and hands-on instructions for the electrochemical etching and the characterisation of PSi. Another book of particular interest is the *Handbook of Porous Silicon* [48]. Its two editions gather reviews written by leading experts in the field of PSi research, covering the fabrication, the properties, the characterisation, the processing and the applications of PSi.

3. Porous membranes fabrication techniques

PSiMs have been fabricated using many different strategies, but all of them can be divided into two categories: the ones relying on electrochemical etching to form the pores, and the ones relying solely on other microfabrication techniques. A summary of PSiM fabrication techniques is presented in Fig. 2.

For the electrochemically etched PSiMs, four different routes can again be distinguished: (1) the anodisation through the entire

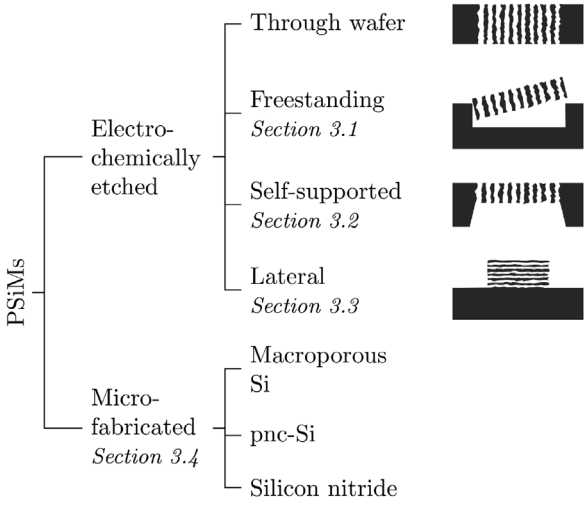

Fig. 2. Summary of porous membranes fabrication techniques.

silicon wafer of standard thickness [55–57,37,58]; (2) the anodisation of part of the silicon wafer and "lift-off" of the porous matrix, creating freestanding PSiMs (see Section 3.1); the fabrication of self-supported PSiMs using anodisation and microfabrication techniques (see Section 3.2); and (4) the creation of lateral PSiMs using anodisation and microfabrication techniques (see Section 3.3). Each approach has its strengths and weaknesses. Through wafer thickness anodisations are very time consuming and results in non-uniform membranes; freestanding membranes are easy to produce but difficult to handle; the fabrication of lateral and self-supported membranes requires the access to microfabrication techniques but their integration into devices is straightforward.

Other approaches that do not rely on electrochemical etching are used to fabricate porous membranes with highly controlled pore geometries. They require techniques such as lithography, dry or wet etching, deposition or annealing. Three different types of non-anodised porous membranes can also be distinguished: macroporous silicon membranes, nanoporous silicon nitride membrane and porous nanocrystalline silicon membranes (pnc-Si). All three types are discussed in further details in Section 3.4.

3.1. Freestanding PSiMs

Freestanding PSiMs are fabricated by electrochemically etching a silicon substrate over a specific area and then consecutively lifting off the porous region. Several approaches exist for the lift off of the membrane. The most common one is the electropolishing of a small cavity below the porous region, by applying one

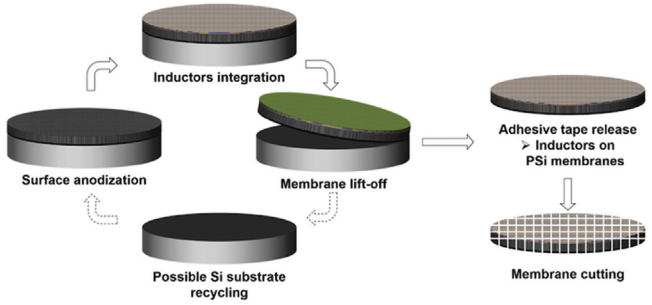

Fig. 3. Illustration of the mechanical detachment of a PSi membrane and the possible recycling of the silicon substrate. Reprinted from [61], Copyright (2018), with permission from Elsevier.

or multiple high current pulses at the end of the electrochemical etch. In order to decrease the amplitude of theses current pulses, the HF content of the electrolyte can be lowered [59]. In another approach, *Preobrazhenskiy et al.* used an alkaline potassium hydroxide (KOH)-based solution for the membrane detachment as it enables an increase in porosity as well [60]. Mechanical detachment is equally possible, by fixing the porous region on tape [61] or polydimethylsiloxane (PDMS)[62], as illustrated in Fig. 3.

Additionally, this figure points out an other advantages of freestanding membranes: the possible recycling of the silicon substrate. It is indeed possible to reuse the same silicon wafer for the fabrication of multiple membranes [61,63]. It is important to note that freestanding PSiMs may however present a strong spatial anisotropy in terms of morphological features. Due to the directionality of the electrochemical etching and the carrier depletion for long etching times, porosity gradients can be observed, either on the surface or deeper in the membrane.

The integration possibilities of freestanding PSiMs are numerous. To establish electric contacts, metals can be deposited on the porous membrane, as illustrated in Fig. 4,(a). These metals include vacuum evaporated gold [64], electroplated copper [60,65] or sputtered indium tin oxide (ITO) [66,64]. For microfluidic integration, PDMS can be cast on top of the still attached PSi films, which then serves as supporting material during detachment [59,67–69]. This method is depicted in Fig. 4,(b). Another integration approach consists simply in the deposition of the membrane on top a specific substrate. This substrate can be another PSi layer [70], a gold slide [71], an ITO slide [72], a glass slide [73–75] or poly(ethylene glycol) diacrylate (PEGDA) matrices [7,14] (see Fig. 4,(c)).

Composite structures can also be fabricated using freestanding PSiMs. *Cencha et al.* constructed an Anodic Aluminium Oxide (AAO)-PSi hybrid membrane relying on capillary forces to firmly attach the PSiMs to the alumina [76]. Other composite structures rely on the deposition of specific materials inside the porous matrix, like the electroless deposition of silver nanoparticles [59,67,68] or the chemical vapour infiltration of graphene [77]. Furthermore, PSiMs can serve as templates for the growth of nanowires, as illustrated by the work of *De La Luz-Merino et al.* [78] in which $CuInSe_2$ was electrodeposited onto glass/transparent conductive oxide (TCO)-supported PSiMs in order to develop novel material for solar cell applications.

3.2. Self-supported PSiMs

Self-supported PSiMs have been developed when the need for robust structures with a high optical quality arose [79]. Freestanding or "etch-through" membranes could not fulfil these needs as they are often characterised by strong spatial anisotropies and porosity gradients. In the "self-supported" manufacturing approach, microfabrication techniques are used to create cavities in the silicon substrate before or after the electrochemical etching. Depending on the doping of the silicon substrate, wet or dry etching techniques are employed.

Fig. 5 illustrates a process employed for the fabrication of self-supported PSiMs using the wet etching on a standard silicon wafer: (a-b) both sides of the wafer are pre-coated with silicon nitride (Si_3N_4) layers and covered with photoresist; (c-d-e-f) the SiN layers are patterned using photo-lithography and buffer oxide etching; (g) the cavity is etched using KOH wet etching until only a few micrometer of silicon remain; (h) the remaining silicon nitride is removed using buffer oxide etching; and (i) electrochemical etching is carried out in order to form the pores. Similar processes have been used in multiple works [28,80–84] and the resulting membranes are similar to the ones represented in Fig. 6, (a–b).

A sacrificial porous silicon layer at the backside can also be used as an alternative to the wet etching [26]. An additional step that is often added to this process is the use of dry etching after the anodisation in order to obtain a fully porous membrane [85]. Indeed, only a few pores open the rear side of the membrane after the electrochemical etching. This can be explained by the fact that, once the first channels reach the backside of the membrane, the current goes through these paths of least resistance and the process stops [86].

Other processes first anodise the silicon wafer over a certain thickness and area, before opening the membranes from the backside. This can be achieved using dry etching techniques like Deep Reactive Ion Etching (DRIE) [88,17,19,79,36,89], as shown in Fig. 6,(c). For this type of process, the oxidation of the PSi prior to the etching is desirable, as this may reduce the etch rate of the porous matrix and create a more uniform membrane. Mechanical grinding is another method used to open the membrane [29,90,91,33,92].

In some works, Silicon-On-Insulator (SOI) substrates are preferred to standard bulk Si, and the top thin Si layer, also called device or active layer, serves as membrane. The handle, which is the thick Si layer, can be opened using wet of dry etching techniques prior to the electrochemical etch [93–95], as depicted in Fig. 7. In this Figure, a single nanopore is formed in the device of the SOI substrate using the following steps: (a-d) fabrication of a Si_3N_4 mask and KOH wet etching of the handle; (e) wet etching of the SiO_2 layer; (f-h) deposition and patterning of a new Si_3N_4 mask; (i-j) patterning of the Si_3N_4 on the device side of the wafer; (k) pre-patterning of the pore using KOH wet etching; and finally (l) the electrochemical etching of the single nanopore. Similar processes can be used to etch membranes with multiple pores [96,97]. The pre-patterning step on the front-side using KOH is also often employed for the creation of macropores, as it induces very regular pore shapes and sizes.

The integration of self-supported PSiMs into devices is more straightforward than for freestanding PSiMs. As they are easier to handle, they can be incorporated into reusable custom-built set ups that can include chambers, channels and electrodes [28,90,91,17,88,97]. For individual integration solutions, PDMS is a good alternative [81,80,19,79]. Others possible substrates are glass slides [24], carbon-paper electrodes [29] or poly(methyl methacrylate) holders [83,84]. Self-supported PSiMs can also be used as substrate onto which the device is transferred [26].

Hybrid structures can be achieved by depositing materials inside the pores, including by the chemical vapour infiltration of graphene [33] or by the growth of carbon nanotubes using thermal chemical vapour deposition [35]. Metals can be coated inside the porous matrix as well. Platinum was immersion plated on PSi to serve as catalyst for micro fuel cell electrodes; since it was deposited before opening the PSi membrane from the backside of the silicon wafer, it also served as etch-stop layer during the plasma etching [30,98]. Other methods which induce electrical conductivity in fuel cell electrodes include the sputtering and electrodeposition of titanium, nickel and gold layers [32].

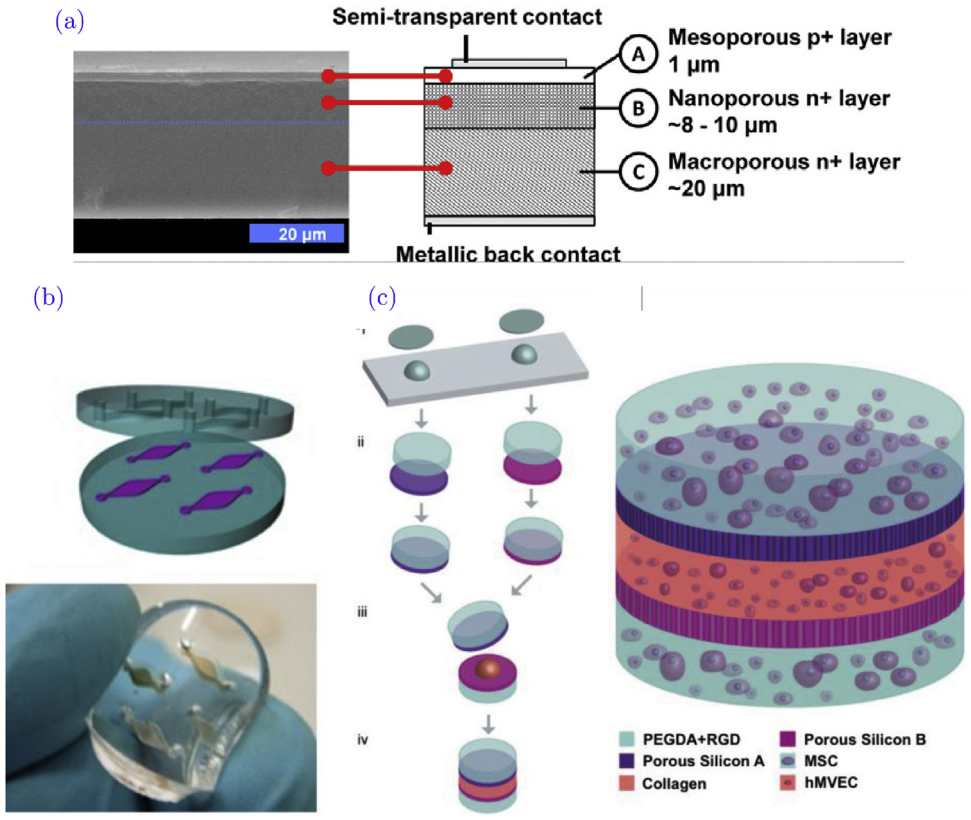

Fig. 4. Examples of freestanding PSi membranes: (a) Integration of a PSiM using vacuum evaporated gold, aluminium and sputtered ITO, reprinted from [64], Copyright (2014), with permission from Elsevier; (b) PDMS-integrated PSiM, reprinted from [67], Copyright (2016), with permission from Royal Society of Chemistry; (c) Integration of two PSiMs with a cell-laden hydrogel and two PEGDA matrices, reprinted from [14], Copyright (2018), with permission from John Wiley and Sons.

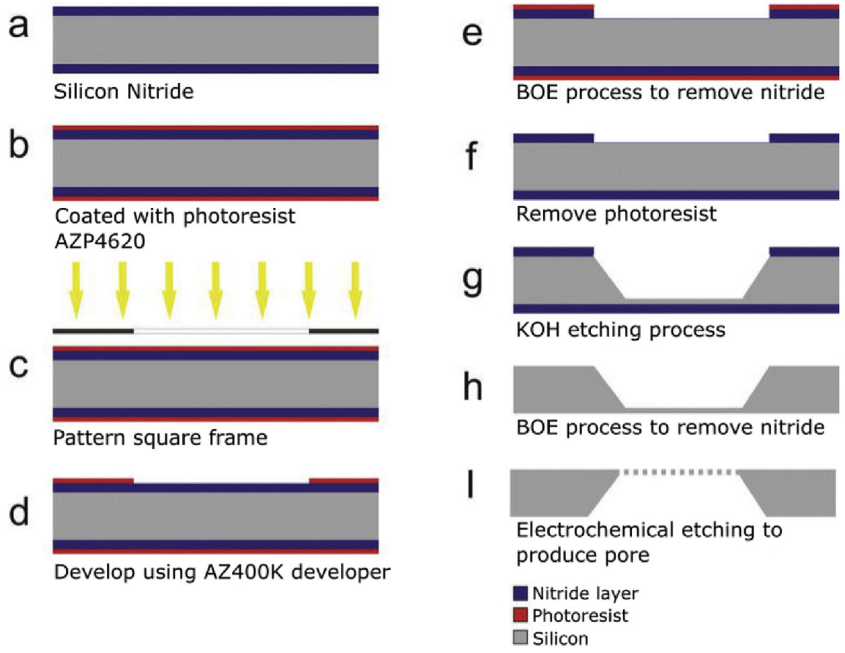

Fig. 5. Fabrication processes for self-supported PSiMs using combinations of dry, wet and electrochemical etching (a) on standard silicon substrates, adapted from [82].

3.3. *Lateral PSiMs*

In order to facilitate the integration of PSiMs, lateral porous membranes have been fabricated using SOI substrates, with pores parallel to the substrate surface [99]. The building process for these lateral PSiMs was developed by *Leichlé* and co-workers and can be divided in four major steps: (1) the micro-channels surrounding the membrane are created using dry etching; (2) the Cr/Au working electrode is deposited and patterned where the anodisation will be initiated; (3) the PSi membrane is created by electrochemical etch-

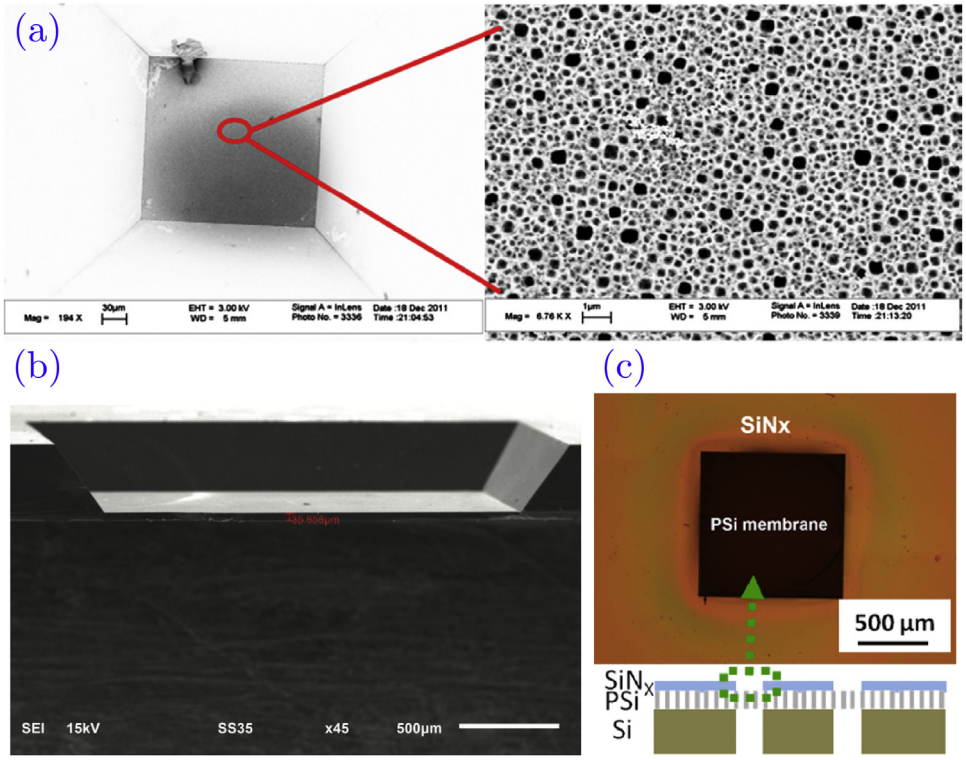

Fig. 6. Examples of self-supported PSiMs(a) Top view of a mesoporous membrane created via wet etching reprinted from [87], Copyright (2013), with permission from Elsevier; (b) Top view of a PSiMs created via wet etching, reprinted from [82]; (c) Top view and schematic view of a PSiMs fabricated using DRIE after anodisation, reprinted from [19], Copyright (2016), with permission from American Chemical Society.

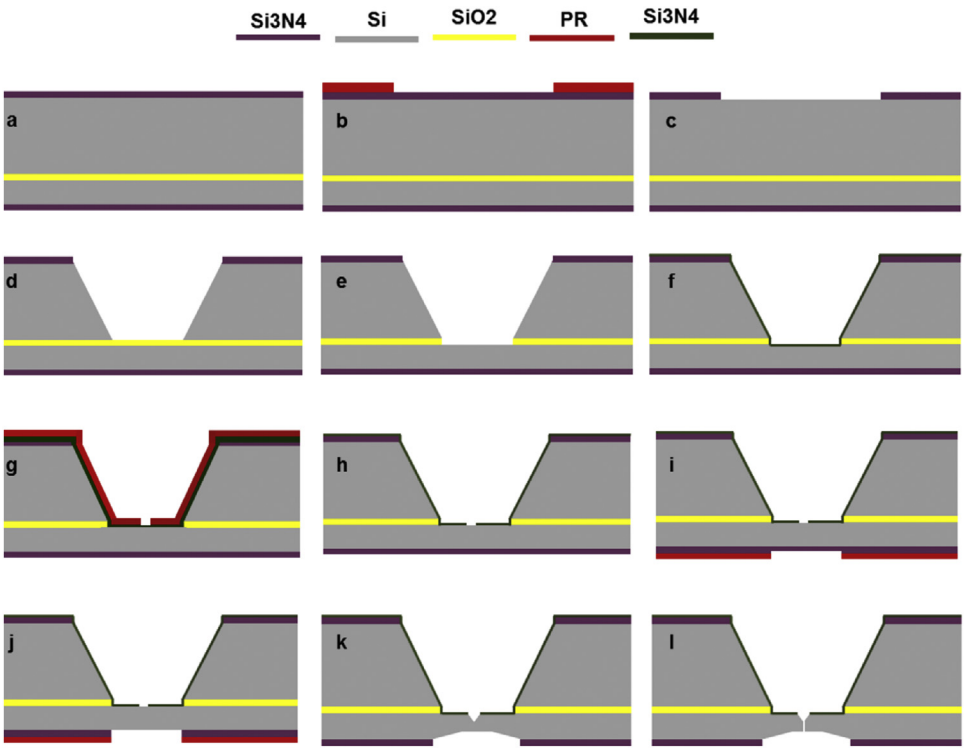

Fig. 7. Fabrication processes for self-supported PSiMs using combinations of dry, wet and electrochemical etching on SOI substrates, reprinted from [93].

ing, using the deposited metal as anode and a Pt wire as cathode; (4) the Cr/Au is removed via wet etching, the fluidic inlet and outlet are made by sandblasting and the chip is encapsulated via anodic bonding.

The resulting device is depicted in Fig. 8. As can be seen in the SEM picture in this figure, the pores are horizontal. This can be explained by the fact that, after their initiation on the membrane sidewall, the pores propagate following the current lines; these cur-

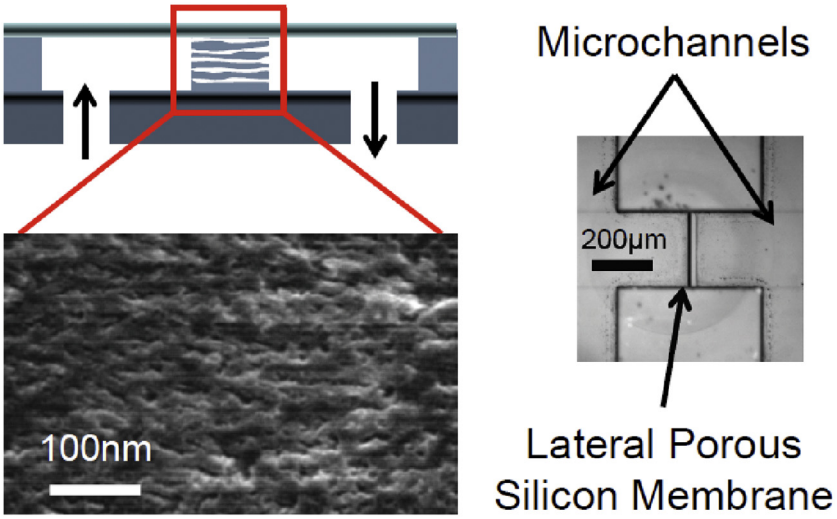

Fig. 8. Schematic view and SEM images from a lateral PSiM, reprinted from [99], Copyright (2015), with permission from Royal Society of Chemistry. In terms of physical properties, the obtained membrane is about 20 µm-high and the pores are 10 µm-long.

rent lines are horizontal, since a metal electrode has been deposited on the opposite side wall.

To improve the process described above and allow the use of standard silicon substrates, ion-implantation can be used in order to define the region of the future membrane [100]. This however puts constraints on the height of such a membrane, which is limited by the thickness of the doping diffusion layer.

3.4. Microfabricated porous membranes

Porous silicon membranes are also prepared without the use of electrochemical etching. To create PSiMs with highly defined geometries, a combination of photolithography and Reactive Ion Etching (RIE) may be used [101,11,16,102,103]. The advantage of this type of process is that the pore size and periodicity can be controlled by the photolithographic pattern, as depicted in Fig. 9,(a). Pore diameters as low as 130 nm can be reached by using a combination of e-beam lithography and DRIE [104–106]. Beside photolithographic mask, block-copolymers have also been used as templates, iron oxide nanodots then serving as "resist mask" to create the pattern via DRIE [107,108]. This method however resulted in many defects in the pore arrangement and pore size distribution.

Directly patterning the channels onto the silicon substrate is nonetheless very time consuming, especially when using e-beam lithography, which has spurred the interest in alternative processes. One of these alternatives is the spontaneous creation of pores during the rapid thermal annealing of amorphous silicon. The thus-formed membranes are called porous nanocrystalline silicon membranes (pnc-Si). The pores originate from the nucleation of nanocrystals inside the amorphous silicon during the rapid thermal anneal [109,111]. As can be seen in Fig. 9,(b), very thin mesoporous membranes can be created using this techniques.

A last type of microfabricated porous membranes, which could be considered as a hybrid form of PSiM, is nanoporous silicon nitride membranes. Theses membranes can be fabricated using the same microfabrication techniques as plain silicon membranes, such as optical lithography and dry etching [13,9,108,112], as depicted in Fig. 9,(c). Focused ion beam (FIB)-milling can be used as an alternative to plasma etching in order to probe holes into the membrane [113,114]. Finally, nanoporous silicon nitride membranes can also be combined with pnc-Si membranes, where the latter serves as template for the dry etching of the nitride layer [109,8,110].

4. Properties

The immense appeal of PSi lies in the alteration of the properties of silicon by the introduction of nano- and microscale porosity into the material. Moreover, these properties are highly tuneable, mostly by fine-tuning the structural features of the porous matrix. By carefully selecting certain morphological parameters, such as porosity, pore size or layer thickness, scientists have been able to adjust the mechanical, electrical, thermal, and biochemical properties of PSi. By detaching PSi layers from their bulk substrate, properties can be altered further, as the effect of the underlying substrate is removed. While the removal of the underlying Si substrate has no effect on the intrinsic properties of PSi, it has an impact of the properties of PSi-based devices. The scope of this impact is detailed in the present section.

4.1. Mechanical properties

Monocrystalline silicon has exceptional mechanical properties: it is fairly hard, characterised by a Knoop hardness of 8.5 GPa (versus 6.5 GPa for steel) [115]; it is remarkably strong but very brittle, which is reflected by a fracture toughness of approximately 1 MPA $\sqrt{m}$ [116]; its yield strength of 7 GPa is higher than that of steel, which ranges from 2 to 4 GPa depending on the variety [1]. However, when silicon is porosified, its mechanical properties are altered. This change depends on the three main morphological features that characterise porous silicon: thickness, porosity, and average pore size. Understanding and optimising the mechanical properties is important for the fabrication of PSiM-based devices, as deformations of the internal structure impact the chemical reactivity and physical properties of the PSi, and the cracking of the membrane affects the durability and operability of the devices. Mechanical properties of PSi and PSiMs must be considered in all the integration schemes developed in Section 3, as the fragility of PSi curtails the number of possible process steps after hte porosification.

The stiffness of PSi is often studied by simulating or fabricating PSi membranes, in order to remove the impact of the underlying bulk Si [117–121]. Both experimental and theoretical results highlight the dependence of the Young's modulus, which quantifies the stiffness, on morphological features: the modulus decreases with increasing porosity and is affected by the pore shape, especially by the presence of branches inside the pores. The evolution

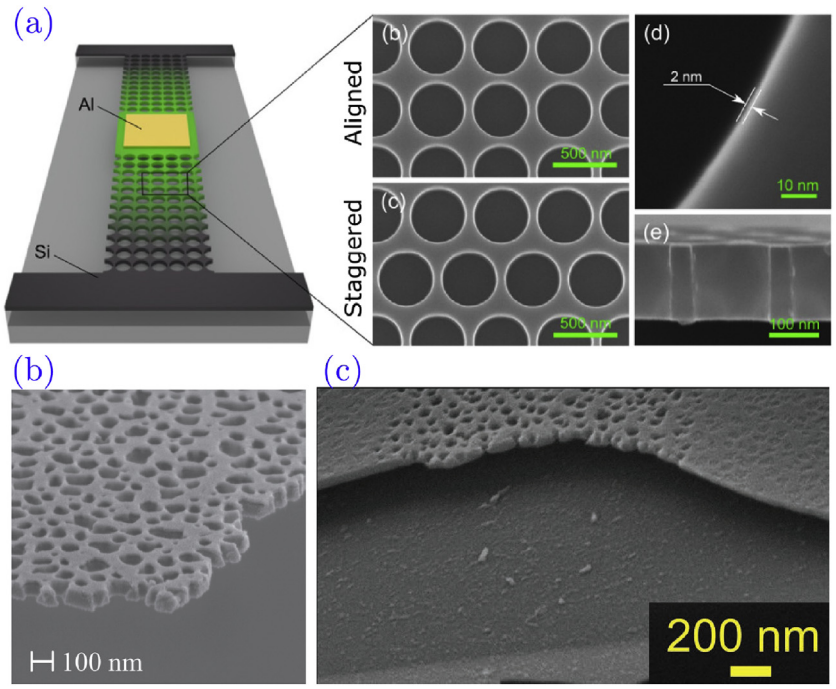

Fig. 9. Microfabricated PSiMs: (a) macroporous membrane prepared using standard microfabrication techniques like e-beam lithography and RIE, reprinted from [105], Copyright (2017), with permission from American Physical Society; (b) pnc-Si membrane, reprinted from [109], Copyright (2017), with permission from Elsevier; (c) nanoporous silicon nitride membrane, reprinted from [110], Copyright (2019), with permission from Elsevier.

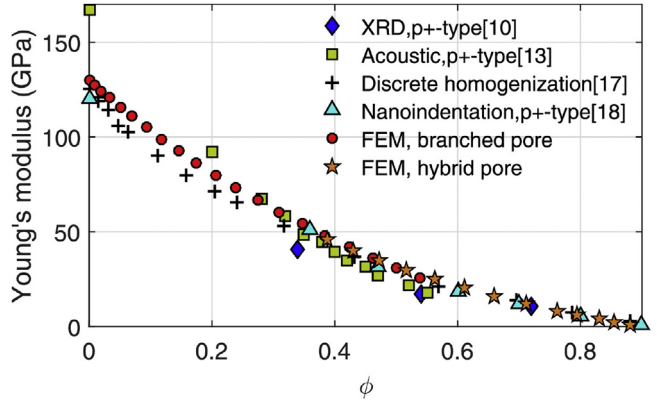

Fig. 10. Evolution of PSiMs Young's modulus with porosity ϕ, obtained both experimentally and via simulations; reprinted from [121], Copyright (2020), with permission from Elsevier.

of the Young's modulus with porosity is illustrated in Fig. 10, in which results from several experimental and finite-element method (FEM)-based studies are compared. A fitting function of Young's modulus E of PSi and PSiMs has been proposed and takes the form of a power law of porosity ϕ, defined as:

$$E_{PSi} = E_{Si}(1-\phi)^m \quad (1)$$

The value of parameter m depends on the geometrical features but is often chosen as $m = 1$ in simulations [109,114]. Other studies prefer the $m = 3$ [122,123] when considering mesoporous silicon. *Gong et al.* [121] modelled this parameter for several types of pore shape, with resulting values fluctuating around $m = 1$ and $m = 2$.

Additional experimental studies concentrate mainly on the residual mechanical stress inside PSiMs [124,123,109]. In *Guider et al.*'s work [124], it was observed that tensile stress is accumulated in the porous silicon layer during the electrochemical etching process. This tensile stress is partially compensated by the underlying substrate. However, when the PSi layer is lifted off the substrate, this stress is released and causes the bending of the PSiM. To quantify tensile residual stress, single bulge test measurements have been used on both pnc-Si and silicon nitride membranes: the fitted values of residual stress are in the order of 10^7-10^8 Pa, depending on the type of membrane [109]. *Dariani et al.*[123] extended the study of residual stress by using X-ray diffraction measurements to inspect the crystal lattice expansion and the perpendicular strain in PSiMs. The internal stress in supported PSi layers was attributed to the slight expansion of the crystal lattice inside PSi and the constraint of the perpendicular planes to the same interatomic spacing as the substrate. When the PSi layer is detached from its substrate, this constraint is released and the perpendicular strain is decreased.

The strength of PSiMs is often analysed via FEM-based simulations of the deflection and Von Mises stress [125,126,114]. It was observed that deflection and stress are dependent on the thickness of the PSiMs: for thick membranes, the deflection and stress are nearly constant with respect to the externally applied pressure; thinner membranes exhibit both higher deflection and stress, which increases with the applied pressure. Reported values of Von Mises stress are in the order of 10^7 Pa for membranes which are a few tens of nanometers thick [125,126]. The total area of the PSiM also has an effect: smaller membranes accumulate less stress and withstand higher pressures. Additionally, pore size and porosity can be tuned to improve mechanical strength, by selecting smaller pore diameters and densities. These theoretical observations were verified experimentally on pnc-Si and nanoporous silicon nitride membranes [109,114].

4.2. Mass transport properties

One of the motives behind the development of open-ended PSiMs was to overcome the diffusion challenges attributed to PSi layers. To verify the added value of membranes, several studies compare the sensitivity of close- and open-ended PSi sensors [21,19,79,69]. The sensing scheme of these studies relies on the adsorption of analyte. Both experimental data and simulations

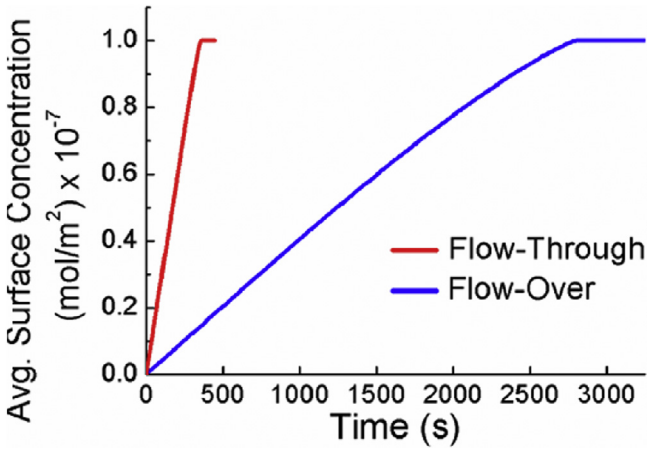

Fig. 11. Simulated average surface concentration of analyte with the same diffusivity, captured by close- and open-ended PSi sensors as a function of time; reprinted from [19], Copyright (2016), with permission from American Chemical Society.

show the increased sensitivity of PSiMs, which means that there is an increase in adsorption. Analyte adsorption has two limiting factors: the transport of the analyte and the adsorption kinetics. In PSi layers, the transport is diffusion-limited, causing a low sensitivity and slow sensor response time. For PSiMs, the transport of mass is influenced by both diffusion and convection, as the analyte flows through the pores, and can be described by the convection-diffusion equation:

$$\frac{\partial c}{\partial t} = \nabla \cdot (D\nabla c - c\mathbf{u}) \tag{2}$$

where c is the analyte concentration, D is the diffusivity and $\mathbf{u}$ is the flow velocity.

An increase of transport leads to an increase of adsorption, which itself translates in a high sensitivity and rapid response time. The increase adsorption capabilities of PSiMs with respect to PSi layer is illustrated in Fig. 11, where the average surface concentration of analyte was simulated for both a PSi layer in flow-over operation mode and a PSiM in flow-through operation mode [19].

The effects of physical properties, such as pore size, membrane thickness and porosity, on the transport of mass inside PSiMs remain to be investigated. Nonetheless, there is a lot of knowledge available concerning mass transport and diffusion on porous materials in general, which might apply to PSiMs as well [127,128].

4.3. Thermal properties

Thermal properties of silicon are also widely altered upon porosification. Porous silicon can exhibit a very low thermal conductivity, which can even become up to 10 times lower when detaching it from its bulk substrate [101]. This unique property has been exploited in specific applications, such as microheaters and temperature-based sensors [48]. For other applications, these thermal properties may be a drawback: for example, when integrating PSi or PSiMs in RF devices, the low thermal conductivity results in the self-heating of the integrated circuit, which is not desirable. This illustrates the importance of understanding how thermal properties are affected by structural features, as the latter can be easily fine-tuned. By carefully selecting the morphology of the PSiMs, a thermal conductivity as low as $\sim 0.9\,Wm^{-1}\,K^{-1}$ and as high as $\sim 55\,Wm^{-1}\,K^{-1}$ can be achieved [56,105]. This represents a decrease of up to two orders of magnitude compared to the thermal conductivity of bulk Si, which equals $150\,Wm^{-1}\,K^{-1}$ at room temperature.

A theoretical investigation of PSiMs' thermal properties demonstrated the influence of physical parameters: thermal conductivity significantly decreased with increasing porosity (by one order of magnitude or more), moderately degrades with increasing pore roughness and is sensitive to pore arrangement [129,130]. The thermal conductivity of PSiMs was experimentally characterised using laser thermometry [101,104,102]. As corroborated by the theoretical studies, the shapes and sizes of the pores were found to strongly affect the thermal properties of the membrane. Thermal conductivity could be reduced by varying the pore diameters and by introducing disorder in the pore arrangement. For high porosity samples, the effect of disorder was found to be more pronounced. This could be explained by the presence of air inside the pores, which dissipated heat. This heat dissipation was tuned by changing the sample-to-volume ratio of the porous structure.

The thermal properties of PSiMs have also been investigated in terms of phonon transport [105,106,131,132,112,130]. Both experimental and theoretical techniques were used and the influence of geometric parameters on phonon transport was highlighted.

Pore geometry was observed to affect the frequency of phonon-boundary scattering events, which reduce thermal conductivity. The effect of pore arrangement was explained by the ballistic phonons, which can propagate over long distances. In ordered pore arrangements, phonons could travel these long distances in a straight line, passing between two rows of pores. In disordered arrangements, such a path is cut off by random pores. This naturally reduces the thermal conductivity. These effects were found to be enhanced at lower temperature, or when the pore diameter is similar to the period.

Valalaki et al. [133] studied the Seebeck coefficient of PSiMs, which characterises the thermoelectric sensitivity of a material. The Seebeck constant was found to strongly depend on porosity. Initially, the coefficient increases with porosity, at this is ascribed to phonon drag and energy filtering effects. The maximum value of $\sim$1 mV/K was measured around 50% porosity, after which the coefficient decreased nearly by half for higher porosities. This reduction is linked to strong scattering effects in the structure, as well as to the reduced carrier diffusion due to confinement and the phonon drag quenching.

4.4. Electrical properties

One of the major electrical properties of PSi is its high resistivity. Depending on the silicon substrate, the structural features, the fabrication and the annealing, the resistivity can be several orders of magnitude higher than the original substrate. For instance, upon electrochemically etching a silicon substrate with an initial resistivity of $10\,m\Omega \cdot cm$, an increase in resistivity of approximately five order of magnitude was observed by *Scheen et al.* [58,134–136]. This increase is explained by the depletion of the free carriers, which itself can be attributed to several phenomena, among which the widening of the energy gap due to quantum confinement and the capture of carriers by traps at the pore surface. Some studies concentrated on PSiMs and qualitatively observed the dependence of resistivity not only on structural properties, but also on the surrounding environment. Indeed, resistivity increases with porosity and membrane thickness [58], but is also affected by pore arrangement [101].

PSi is also characterised by a low permittivity: by porosifying a silicon wafer over its full thickness, its effective permittivity goes from 11.7 to $\sim$5.4 (for 50% porosity) or $\sim$3.6 (for 70% porosity) [134,58,135]. Thanks to its high value of effective resistivity and low permittivity, PSi is a semiconductor substrate which introduces low electromagnetic losses, reduced parasitic coupling (crosstalk) and vanishes the signal harmonics distortion (reduction of more than 100 dB) [58,134–136].

The effect of temperature on electrical properties is more complex and requires more investigations. *Hagino et al.* [101] reported that resistance slightly increases with temperature based on measurement carried from −100 °C to 60 °C, while [58] outlined a significant decrease in resistivity of two orders of magnitude for temperatures of 150 °C or higher. *Rack et al.* [136] observed both trends for different PSi layers in the same temperature range and hypothesised that the structural properties of the porous structure influence the impact of temperature on resistivity.

4.5. Optical and optoelectronic properties

The peculiar optical properties of PSi have been the subject of multiple studies and applications [48,54]. These optical properties can be tuned in a wide range, depending for example on the pore size, which can be smaller than the optical wavelength. One of the main optical parameters of PSi, namely its refractive index, can be fine-tuned by adapting the porosity. Variations of the refractive index within a PSi membrane create specific structures, like Bragg stacks, microcavities and rugate filters [137,62,7,76,138,74,75]. Photoluminescence is also another major optical property of PSi, which is conserved when fabricating PSiMs [72]. The study of the optical properties of PSi and PSiMs often involves reflection and transmission measurement techniques. An accurate assessment is however not as straightforward since surface roughness and morphological inhomogeneities must be taken into account [54].

Reflection and transmission techniques can also be used to study optoelectronic properties of PSi and PSiMs, such as free carrier lifetime for example. Among these techniques are time resolved pump-probe transmission and reflection measurements, which have been used to study the dielectric function and the carrier dynamics inside PSiMs [139–143]. Pump excitation induces the optical activation of free carriers, which then modify the dielectric function of the silicon skeleton of the membrane. This modification is however non-uniform, which can be easily explained: the laser pulse intensity drops when it propagates into the depth of the membrane; since free carriers reproduce the absorption of this pulse, the optical response is also depth-dependent. A model was developed by *He et al.* [139] to retrieve the change of the dielectric function based on the membrane depth. This model was then used in later work in order to map the time-dependent spatial distribution of free carriers [143]. It was found that Shockley-Read-Hall and Auger recombination governs the carrier's dynamics, while diffusion is insignificant. Constants related to excited charge transport, such as the recombination time and the carrier diffusion constant were also been modelled and studied [140,143].

Zakar et al. [141,142] complemented these findings and refined the analysis of the Auger recombination mechanism, which was found to amplify at the wavelength matching the infrared (IR)-active vibrational modes of the molecular impurities present on the pore's surface. These uncovering's were partly supported by *Park et al.* [144], as they found that a PSiM exhibits high transparency properties in the mid-wavelength infrared (MWIR) spectrum, while being strongly absorptive for shorter and longer wavelengths. The absorptive properties are linked to vibrational mode from surface's impurities. The transparency of the PSiM could be modulated by external optical excitation, demonstrating the possible application of PSiMs as optical intensity modulators [144,142]. Upon external optical excitation, excited free charge carriers interact with the MWIR signal, and transmittance is reduced. This decrease can reach up to ∼50% and last from a few tens to a few hundreds of pico-seconds, all depending on the porosity, pore size and thickness.

4.6. Biochemical properties

PSi is often used in biomedical applications because of its biocompatibility [48]. Freshly etched PSi is naturally biodegradable in physiological solutions. The hybrid silicon structure covering the surface of the pore is very reactive and quickly oxidises when in the presence of water. Depending on the pH, this oxide can then react with water to form silicic acid, as described in the following reactions:

$$Si + 2H_2O \rightarrow SiO_2 + 2H_2 \quad (3)$$

$$SiO_2 + 2H_2O \rightleftharpoons Si(OH)_4 \quad (4)$$

This oxidative hydrolysis reaction is stable at low pH, but highly corrosive at high pH [145]. At physiological pH, there is only a slow dissolution of the porous layer. For some applications, the degradation of PSi in aqueous solutions is however unwanted and solutions to improve the stability have been investigated. The solutions are numerous for PSi layers and include among others thermal oxidation [146], hydrosilylation [147], atomic layer deposition [148] and thermal hydrocarbonisation [149].

Some of theses techniques can not be transferred to PSiMs, like thermal stabilisation for example: thermal oxidation causes the expansion of the porous structure, and is mesoporous PSiMs, this causes the physical deformation and sometimes even degradation of the membranes [89]. *Baraket et al.* [89] studied alternatives for thermal stabilisation and found that the chemical etching using standard cleaning procedures RCA1 and RCA2, combined with silanisation, offered the best stability in physiological media while preserving the integrity and the biocompatibility of the PSiMs.

Oxidation is not always the preferred method of stabilisation, especially for long term applications. In such cases, more adequate methods, such as thermal hydrocarbonisation [18], silanisation [12] or hydrosilylation [14] are easily applied to PSiMs. Hydrocarbonisation however compromises the biocompatibility of the membrane, and remedies were investigated: by simply pre-incubating thermally hydrocarbonised PSiMs in physiological media, the biocompatibility was recovered [18].

5. Applications

The main applications of PSi membranes can be divided into five domains: microfluidics, medical applications, sensing, energy conversion and electronics. Table 1 categorises the applications of PSiM-based devices covered by this review. All these applications utilise PSiMs instead of other substrates because of one or several of their unique properties. It is however important to note that some of the other properties of PSiMs may form obstacles to the introduction of those devices to the market. For instance, the lack of mechanical stability is a major hindrance for many applications, which encourages the thorough study of all parameters affecting the mechanical properties of PSiMs.

Microfluidics take advantage of the structural properties of PSiMs. The most common applications is filtration, which makes use of the open-ended pores. As pore size can easily be controlled during the fabrication process, filtration in PSiMs is most often size based [99,151,152,100,81]. For these applications, mesoporous membranes are used, meaning that only small nanometer-sized molecules can pass through the filter. Charge-based filtration is also possible since the membrane can exhibit a certain permselectivity in the presence of a charged buffer and an electric field [152].

As discussed in Section 4.6, PSiMs are used in the field of biomedical science because of their biocompatibility. PSiMs are mostly used as scaffolds for cell culture and tissue engineering. More details about these applications will be outlined in Section 5.1. Other biomedical applications include drug delivery patches [7],

Table 1
Recent advances in the applications fields of porous silicon membranes (*Note: C, F, FT, L, M, S stand for, respectively, Commercial, Freestanding, Full Thickness, Lateral, Microfabricated and Self-supported.*)

Application field	Membrane characteristics	Membrane thickness	Detailed application	Ref.
Microfluidics	M, mesoporous	15 nm	Size and charge selective filtration	[150]
	S, mesoporous	5 μm	Filtration of small biological molecules from mixtures	[81]
	L, mesoporous	10 – 20 μm	Size and charge selective filtration	[99,151,152,100,153]
	S, macroporous	215 μm	Electro-osmotic pump	[90]
Medical	F, macroporous	4.29 μm	Drug delivery patch and optical monitoring of drug release	[7]
	M, macroporous	50-60 nm	Culture of human umbilical vein vascular endothelial cells	[8]
	M, macroporous	500 nm	Reconstruction of the intestinal barrier of a trout via cell culture	[9]
	M, mesoporous	75 nm	Small-format hemodialysis with high toxin elimination capabilities	[10]
	M, macroporous	30 μm	Transmigration assay for cancer cells	[11]
	F, mesoporous	276 μm	Scaffold for the culture of oral mucosal epithelial cells	[12]
	C, macroporous	1 – 10 μm	Support for the investigation of pore-spanning lipid membranes	[154–160]
	M, mesoporous	30 nm	Cell culture of endothelial cells	[13]
	F, macroporous	12 – 15 μm	Tissue scaffold integrated with cell-laden hydrogel biomaterials	[14]
	M, macroporous	5 μm	Lung-on-chip microfluidic device	[15,161]
	M, macroporous	10 μm	Culture of intestinal epithelial cells	[16]
	S, macroporous	130 – 150 μm	Mechanical cell lysis and DNA isolation	[17,88]
	F, mesoporous	4 – 5 μm	Implantable scaffold for cell culture	[18]
Sensing	S, macroporous	~50 μm	Electrophysical NO_2-gas detector	[85]
	F, mesoporous	1.7 μm	Silver-modified sensor for SERS-based detection of miRNA	[59]
	L, mesoporous	10 μm	Interferometric transducer for solvent detection	[153]
	F, mesoporous	1.6 μm	Optical detection of ethanol vapour	[138]
	S, mesoporous	2.5 μm	Impedance spectroscopy of the formation of a lipid membrane	[94,95]
	F, mesoporous	29 μm	Electrostatic isopropanol vapour sensor	[20]
	F, mesomacroporous	5.5 μm	Optical detection of Bovine Serum Albumin	[21]
	F, mesoporous	17 – 21 μm	Optical detection of dissolved gas concentrations in liquids	[137]
	M, mesoporous	50 nm	Nanopore-based sensing of DNA translocation	[110]
	S, mesoporous	20 μm	Multi-assay solvent vapour optical detection	[162]
	F, mesoporous	870 nm	Multianalyte detection using silver-decorated sensors	[67,68]
	M, mesoporous	15 nm	Optical detection of Bovine Serum Albumin permeation	[22]
	F, mesomacroporous	4.5 μm	Electrochemical detection of MS2 bacteriophage	[71]
	F, mesomacroporous	4.5 μm	Label-free electrochemical detection of bacterial toxin	[163]
	M, mesomacroporous	50 nm	Electrochemical detection of ion-transfer across the PSiM	[113]
	C, macroporous	475 μm	3D liquid core sensor array	[164]
	S, mesoporous	340 nm	DNA translocation detection	[96,97]
	M, macroporous	50 μm	Immunoassay for specific leukocyte subsets	[103]
	S, macroporous	1 – 3 μm	Transmembranes proteins sensing	[87]
	C, mesomacroporous	10-15 nm	DNA translocation detection	[165–167]
	F, mesoporous	19.9 μm	Optical aptasensors with multiple target-binding sites	[23]
	S, mesoporous	4 – 15 μm	Optical detection of enzyme adsorption and streptadivin binding	[19,79,168]
Energy conversion	F, micro/macroporous	10 – 30 μm	Wide-gap absorber for solar cells	[66,64]
	S, mesoporous	~70 μm	Implantable glucose biofuel cell	[89]
	S, mesoporous	5 – 20 μm	Ion-exchange membrane for micro fuel cells	[27]
	S, mesoporous	50 μm	Anion exchange membrane for Glucose/O_2 micro fuel cell	[28]
	S, macroporous	125 μm	Membrane-electrode assembly for H_2/air-fed micro fuel cells	[29]
	S, macroporous	230 μm	Microfluidic electric generator	[91]
	S, mesoporous	13 μm	Monolithic Si electrode for micro fuel cells	[30,98]
	F, macroporous	50 μm	Anode for lithium-ion batteries	[63,60,65]
	F, mesoporous	200 μm	Anode for lithium-ion batteries	[31]
	M, macroporous	5 μm	Electrode grids for micro fuel cells	[32]
	S, micro/macroporous	210 μm	High-conductivity electrodes for micro fuel cells	[33]
	M, macroporous	280 μm	Ion-exchange membrane for photoelectrochemical cell	[34]
	S, macroporous	50 μm	Electrode for methanol micro fuel cell	[35]
	S, macroporous	60 μm	Cathode for self-breathing microfuel cells	[36]
	FT, meso/macroporous	500 μm	Membrane-electrode assembly for hydrogen/oxygen micro fuel cells	[57,37]
	S, mesoporous	100 μm	Proton exchange membrane for methanol micro fuel cells	[83,84]
	S, meso/macroporous	80 – 100 μm	Pervaporation membrane for methanol vapour-fed micro fuel cells	[80]
Electronics	F, mesoporous	46 μm	RF insulating and supporting substrate for microfabricated inductors	[61]
	S, mesoporous	10 μm	MEMS-based superheated loop heat pipes	[24]
	M, macroporous	600 nm	Thermal management device	[25]
	S, mesoporous	300 μm	Thermal isolation layer for high temperature micro-hotplates	[26]
	F, macroporous	2.46 μm	Flexible optoelectronics device	[72]
	F, mesoporous	1.92 μm	Modulator for photodetector	[74,75]
	FT, mesoporous	380 μm	CMOS compatible RF insulating substrate	[58]

hemodialysis membranes [10], DNA purification devices [17,88] or supports for the investigation of pore-spanning lipid membranes [154–160].

Sensing and diagnostics are the most common application fields of PSiMs, especially of mesoporous PSiMs. This can be explained by the physical, optical, mass transport and biochemical properties of the membranes: analyte solutions can flow through the membrane; target molecules can be retained, based either on their size or on interactions with the pore walls, and both flow and immobilisation can be detected by a change in the optical properties of the membranes. PSiM sensors can be divided into two categories: gas sensors and biosensors. Gas sensors often detect the presence of solvent vapours [20,138,153]. PSiM-based biosensors have been fabricated for many target molecules, which will be detailed in Section 5.2.

The electrical properties and permselectivity of PSi encouraged its use in the area of energetics. A recurrent use for PSiMs is therefore as base material for microfuel cells [169]. This will be discussed in more detail in Section 5.3. PSiMs are also used as anodes for lithium-ion batteries, since they have many advantages: they form an alloy of $Li_{22}Si_5$, resulting in a very high capacity; they have a very low discharge potential; by tuning the physical properties, they can withstand many charge/discharge cycles; and finally, they are cost-effective [170,63]. An exhaustive list of PSiM applications for Li-ion battery anodes is detailed by *Luais et al.* [171].

The last area of applications considered in this review is electronics. The low thermal conductivity of PSiMs (see 4.3) renders them ideal substrates for thermal devices such as micro-heaters [24,26,25]. PSi is also used for RF isolation, in the form of layers or membranes [61]. The interest of PSi for RF applications originates from its lower effective resistivity and permittivity compared to bulk silicon which translate to a silicon-based substrate which is characterised by lower electromagnetic losses, reduced crosstalk and much weaker signal harmonics distortion. The low thermal conductivity is however a hindrance for RF application, as it causes the integrated circuit to self-heat. Other microelectronic-related applications include optelectronic devices, like wavelength modulators [144] or light emitting capacitors [72].

5.1. Tissue engineering scaffolds

The interest in PSiMs for regenerative science emerged because of its many biochemical properties: as detailed in Section 4.6, they are inorganic, biocompatible *in vitro* as well as biodegradable *in vivo*. Other attractive capabilities include the many possible surface modifications and the possibility to load cells or drugs inside the porous matrix.

Nehilla et al. [13] used pnc-Si membranes to grow mouse and human endothelial cells. It was observed that the permeability of the membrane influences the cell maturation and morphogenesis: firstly, unstained "holes", called vacuoles, were observed with the cells and secondly the cells arranged themselves into capillary-like structures and branched networks according to the membrane's geometry. Vacuole expression is not specific to pnc-Si membranes and was observed on microfabricated silicon nitride membranes as well. It was however observed that untreated silicon nitride does not promote cells adhesion as well as pnc-Si membranes, as the culture of endothelial cells is delayed on silicon nitride membranes [8]. Surface functionalisation is therefore essential, not only for regenerative sciences but also for other biomedical applications. *Drieschner et al.* [9] coated their porous silicon nitride membrane with fibronectin before culturing trout intestinal cells, in order to promote cell adhesion. By growing both epithelial cells and fibroblasts, the intestinal wall could be mimicked and the effect of physiological signals could be modelled. A similar study was performed earlier by *Sajay et al.* [16] using microfabricated PSiMs and human intestinal epithelial cells. By continuously infusing liquid through the membrane, the cells were able to differentiate in morphology: the cell displayed a columnar geometry, which depended on the PSiM's geometry as well. The obtained structure provided a good model for the human intestinal barrier, which makes it possible to study important cellular functions of the intestine.

Microfabricated PSiMs were integrated into a Boyden chamber by *Hosseini et al.* [11] in order to study the transmigration of cancer cells. Human breast cancer cells were cultured and their migration was monitored under different conditions. It was observed that the cells are capable of migrating to the underside of the membrane where serum is present in the media. Additionally, the migration of drug-treated cells was investigated and was found to be quasi inexistent. *Punde et al.* [15] microfabricated PSiMs and integrated them into "lung-on-chip" microfluidic devices. They co-cultured

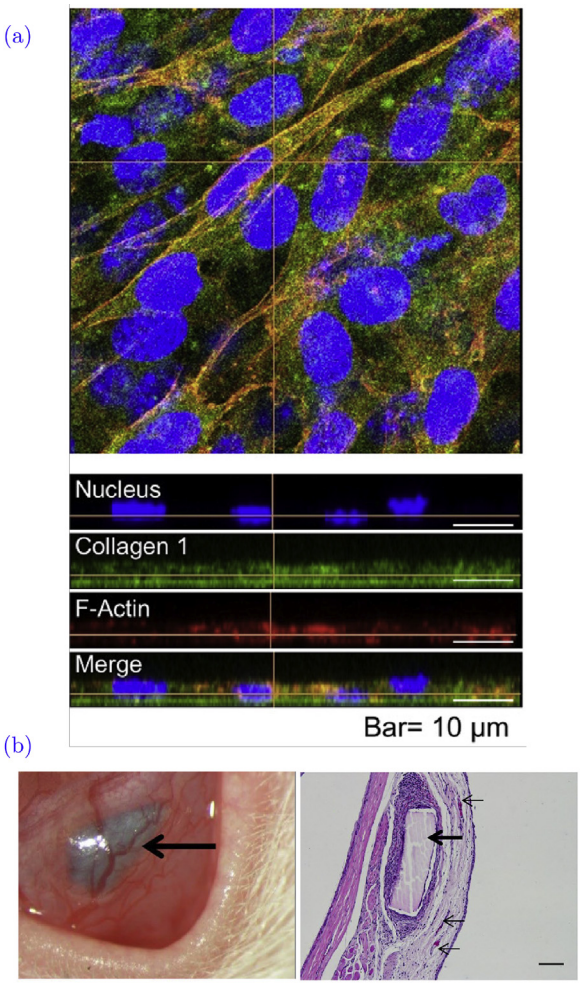

Fig. 12. Examples of PSiM-based schaffold for cell culture: (a) Formation on fibroblast on a pre-incubated thermo-hydrocarbonised PSiM, reprinted from [18], Copyright (2016), with permission from Elsevier; (b) collagen-functionalised PSiM implanted in a rat's conjuctiva for the culture of oral mucosal epithelial cells, reprinted from [12].

different cells on the PSiMs, mimicking the bronchial epithelial lining in order to investigate the role of eosinophil cationic protein in lung inflammation. Their model could however also be used to study the effect of flow conditions on cell migration and cell-cell interactions [161].

Electrochemically etched PSiMs can be used as scaffold for cells culture as well. *Tong et al.* [18] demonstrated the pre-incubation in Phosphate-buffered saline (PBS) for 10 days solves the cytotoxicity problems encountered with thermally hydrocarbonised PSiMs. Mouse embryonic fibroblastic cells successfully grew on the membrane, as illustrated in Fig. 12,(a). As the membrane structure was characterised as a rugate filter, the cell culture could be optically monitored. The *in vivo* performance of the scaffold were further investigated in a murine model. The pre-incubated PSiMs exhibited no cell necrosis or inflammation in the vicinity of the implant, demonstrating that PSiMs can be used simultaneously as an implant for cells culture or drugs delivery and as a subcutaneous optical biosensor. *Irani et al.* [12] tested a different functionalisation method for implantable PSiMs: the membranes were coated using collagen-IV and vitronectin after oxidation and aminosilanisation. Male origin-rat oral mucosal epithelial cells were cultured on the scaffold, which was then inserted in a rat's conjunctiva in order to serve as bandages for the purpose of ocular repair. Signs of inflammation could be observed around the implant, as can be

observed in Fig. 12,(b). There were additional indications hinting to the partial degradation of the membrane. Although the membranes seemed well tolerated, improvement is possible. No cell migration was observed from the implant to the host, but this may be linked to the fact the corneas were not wounded and no cell repair was needed.

A final approach to using PSiMs as scaffolds for cells culture and regenerative science was provided by *Pei et al.* [14]. The PSiMs are stacked with cell-laden hydrogels in order to form a vertical integration that simulates native tissue architectures. In most solid native tissues, membranes both promote cell adhesion and modulate diffusion between other layers of the tissues. In the 3D-scaffold, each PSiM had specific photonic properties, which allowed the optical monitoring of the biomaterial. One membrane tracked the secretion of enzymes by the cells present in the adjacent hydrogels. The other scaffold was loaded with a bioactive compound as well, of which the release was optically supervised. As each film had distinct optical features, these two phenomena could be monitored simultaneously.

5.2. Biosensors

Biosensing is a very widespread use of PSi. This is linked to the large surface area and many physical and chemical properties of the porous matrix [172]. Most PSi biosensors rely on changes in the optical features as means of detection, like for example a shift in the reflection spectrum or the quenching of the photoluminescence [173–175]. Other detection methods include impedance or amperometric sensing [176]. As per definition, biosensors are not only composed of a detection element or transducer; they further include a recognition element to capture the analyte. This element can take the form of antibodies, antigens, enzymes, complementary DNA, and so on. For PSi layers, the capture of analyte is however often limited, which is why PSiMs are more alluring for biosensing application. As detailed in Section 4.2, multiple comparative studies between PSi layer and PSi membranes have show the advantages of the latter in terms of biosensing: the sensitivity is increased and the response time is shortened [79,19,69,23].

Most PSiM-based biosensors rely on optical detection schemes. *Kumar et al.* [21] fabricated freestanding PSi microcavities for the detection of Bovine Serum Albumin (BSA). The recognition element of the biosensor was introduced via functionalisation: (3-Aminopropyl)triethoxysilane (APTES) was first used to provide amine terminations to the oxidised PSi, onto which glutaraldehydes were grafted. When BSA is captured inside the porous matrix by the glutaraldehydes, the refractive index of PSi increases and the optical signal shifts to higher wavelengths. The detection therefore consists in monitoring the shift of the microcavity resonance wavelength. *Zhao et al.* [19] used a similar photonic structure for their biosensor, but made the membrane self-supported in order to reduce the risk of surface inhomogeneities and mechanical failure. The sensor was APTES- and biotin-modified. The detection relied on the red-shift of the microcavity resonance wavelength upon streptavidin adsorption. The total detection time amounted to 20 minutes, which was 6 times faster than for a PSi layer-based biosensor, thus demonstrating the improved mass transport and the increased analyte capture of open-ended PSi films described in Section 4.2. The monitoring of photonic optical features is used in biomedical applications as well, where sensing is not the only role of the PSiM. Optical biosensing is used to track drug delivery [7], cellular secretion and biomolecular release [14] as well as to report *in vivo* cell and tissue responses [18].

Not all optical biosensors rely on photonic structures for the detection of biomolecules: the monitoring of the effective optical thickness (EOT) is also possible, although it requires some post-processing of the recorded optical spectra. The EOT is linked to the average refractive index (n) and the PSi thickness (L) by the following equation: $EOT = 2nL$. *Yu et al.* [23] used the relative EOT to track the binding of thrombin to aptamer, using the data post-processing method developed by *Barillaro* and co-workers [177]. The biosensor consisted in a mesoporous freestanding PSiM, functionalised with thrombin-binding aptamers. The detection performance and selectivity of the sensor can be observed in Fig. 13,(a).

Surface-enhanced Raman spectroscopy (SERS) is another optical method that can be used to detect biomolecules. It measures the Raman scattering of molecules, which is enhanced by the resonant excitation of surface plasmons in adjacent metal nanostructures. Underneath the metal nanoparticles, a dielectric substrate is preferred to increase the sensor sensitivity. PSiMs were found to be promising supports for such biosensors [59]. PDMS was used as mechanical reinforcement, and silver nanoparticles were deposited onto the porous surface by inkjet printing or by immersion plating. A DNA probe was attached to the nanoparticles as recognition element. The thus-fabricated biosensor was able to detect the target miRNA with a sensitivity comparable to commercial techniques. The potential of the chip as multiplexing biosensing platform was studied in further works [67,68]. Polyadenine (polyA), polyguanine (polyG), polythymine (polyT) and polycytosine (polyC) solutions were injected in the four chambers of the biosensing platform, respectively. The SERS spectra measured for each chamber can be seen in Fig. 13,(b). The fingerprint of each DNA nucleobase can be easily recognized.

Besides optical detection methods, biosensors can also rely on electrical characterisations as means of diagnosis. *Reta et al.* [71] used differential pulse voltammetry (DPV) to probe the binding bacteriophages or bacterial toxin on the pore walls. As illustrated in Fig. 13,(c), the biosensor consisted of an antibody-functionalised freestanding PSiM, deposited onto a gold slide. When the target biomolecules bound to the antibody, the pores became partially blocked. The blockage hindered the diffusion of electroactive species present in the solution to the gold slide, which resulted in a decrease in the current intensity. The thus-constructed platform formed a simple, direct and sensitive biosensor, and allowed for example the indirect detection of gram-negative bacteria, down to 1 CFU/mL [163].

A final category for PSiM-based biosensors concerns nanopore-based sensors. The most common target for such sensors is DNA sequencing, which traditionally relies on ionic current measurements. This approach has a major drawback: the high speed of DNA translocation prevents the accurate detection of the current alternations identifying the individual bases. To address this challenge, *Madejski et al.*[110] designed a nanocavity, capped with a nanoporous silicon nitride membrane, to preconfine the DNA. During this preconfinement, the DNA strands are stretched, which results in a lower speed of translocation. Another strategy to reduce translocation speed consists in the construction of high aspect nanopores [96]. Moreover, this method enables the fabrication of a nanopore array for simultaneous DNA sequencing. By attaching fluorophores to the DNA strands, translocation events can be detected optically using a microscope and a laser excitation [97]. *Yamazaki et al.*[165–167,178] also optically observed DNA translocation using commercially PSiMs. Fluorescent probes were attached to the DNA strands and excited by ultraviolet light. This method could be used to replace ionic current-based DNA sequencing: fluorescent labels identifying each base separately could be attached to the DNA strand and each base could be discriminated using single-photon counting methods. Such counting methods seem very promising and have already been found to reliably measure the permeation of BSA through pnc-Si membranes [22].

Another application of PSi nanopore-based sensors was developed by *Kahn et al.* [93–95]. Their nanopore membranes were functionalised with a lipid membrane. Additionally, an epithelial

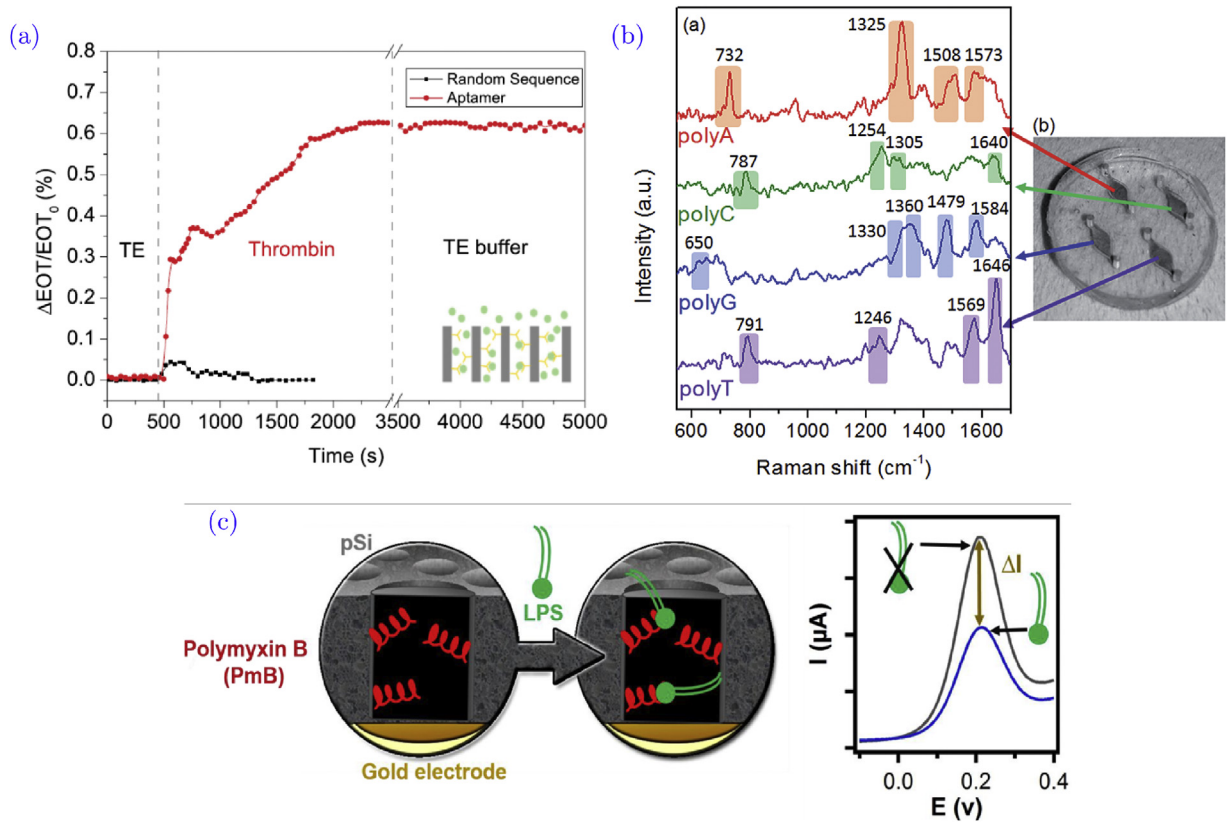

Fig. 13. Examples of PSiM-based biosensors: (a) detection performance of aptamer-modified optical biosensors, relying on the increase of relative effective optical thickness upon thrombin binding, reprinted from [23], Copyright (2019), with permission from Elsevier; (b) SERS spectra for multianalyte detection on four different silver nanoparticles-decorated PSiMs, reprinted from [67], Copyright (2016), with permission from Royal Society of Chemistry; (c) sensing principle of a voltametric PSiM-on-gold biosensor, and corresponding differential pulse voltammetry (DPV) traces before and after the binding of lipopolysccharides (LPS) bacterial toxins, reprinted from [163], Copyright (2019), with permission from American Chemical Society.

sodium channel was embedded into some of the fully formed artificial lipid membranes. The functionalities of both lipid membrane and channel protein were analysed using electrochemical impedance spectroscopy. The platform exhibited long-term stability, making it a promising tool for the study of ion channel electrophysiology.

5.3. Micro fuel cells

With the rise of the Internet of Things, portable devices integrate more and more complex functions, which inevitably increase their power consumption. This trend encouraged the interest in miniaturised fuel cells as energy source, replacing the lifetime-limited batteries. A fuel cell converts chemical energy into electrical energy. It is made of two electrodes, which are in contact with an electrolyte. The system can be qualified as an electrochemical energy source, since an oxidation and a reduction reaction occur at the electrodes. At the anode, the fuel is oxidised by a catalyst, releasing cations and electrons. Electrons will create the electric current, while cations will diffuse through the electrolyte to the cathode. There, the cations recombine with the electrons and react with an oxidising agent. The most common fuel used is hydrogen, and the oxidising agent is often oxygen. For the system to operate, fuel and an oxidising agent must be provided to the reactor chamber. Another requirement rests on the permselectivity of the electrolyte, which must only allow the passage of positively charged ions. This is why an ion-exchange membrane is often used to separate the electrodes. A gas diffusion layer can also be added to the stack in order to distribute the fuel on the catalyst layer [48].

Porous silicon membranes have been found to be a promising candidate as base material for micro fuel cells [169]. It can be used for fuel supply, serve as ion-exchange membrane or can be integrated in the core system, either as part of a membrane electrode assembly (MEA), as gas diffusion layer or as catalyst support.

Wu et al. [80] used mesoporous PSiMs in their methanol fuel cell. While conventional methanol fuel cells are often liquid-fed, vapour-fed ones have the advantages of a lower methanol crossover and a higher fuel efficiency. PSiMs were therefore used as pervaporation membranes for fuel supply. Another type of fuel cells, which is more and more studied, is glucose fuel cells. Glucose is present in many organisms, and such fuel cells could therefore easily power implanted medical devices. PSiMs could be used for the fuel supply in these implanted biofuel cell: it would allow small molecules and ions to pass through, but prevent the infiltration of antibodies and cytokines, as illustrated in Fig. 14,(a). With this application in mind, *Baraket et al*[89] developed a stabilisation method for PSiMs in physiological media. This method did not impact the diffusion properties of the membranes.

The use of PSiM as ion-exchange membranes for fuel cells has long been studied [169]. While some works concentrate more on the fabrication of the membrane [27], most studies [28,84] focus on the functionalisation, which is required to make the membrane electrically isolating but ion permeable. *Haddad et al.* [28] grafted quaternary ammonium functions to hydroxylated PSiMs in order to enhance the diffusion of anions in glucose/air fuel cells. For methanol micro fuel cells, the functionalisation using sulfonic acid groups was observed to induce proton conductivity [83,84]. For both types of fuel cell, the performance of the membrane was superior to Nafion® membranes, which are traditionally used as

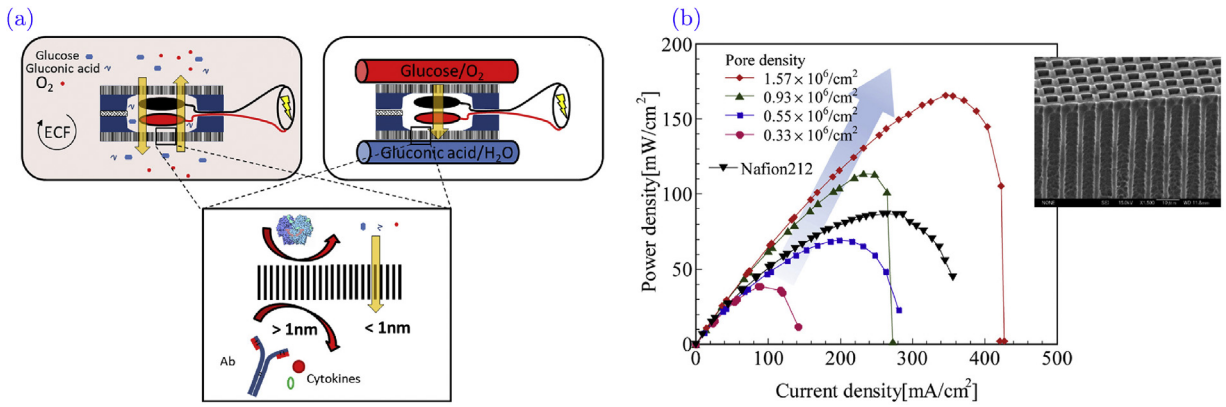

Fig. 14. Examples of micro fuel cells and their performance: (a) glucose micro fuel cell for the power supply of implanted medical devices, reprinted from [89], Copyright (2020), with permission from Elsevier; (b) performance of a PSiM-based MEA in a hydrogen micro fuel cell, reprinted from [29], Copyright (2014), with permission from Elsevier.

ion-exchange membrane. PSiMs are also more cost-effective than Nafion® membranes, making it a promising alternative for next-generation micro fuel cells. *Nagayama et al.*[29] integrated their PSiM to a MEA: after electrolyte filling, the PSiM was sandwiched between two catalyst-coated carbon-paper electrodes. The performance of the fuel cell was investigated, with increasing pore density. The PSiM-based MEA with pore densities of 10^6 pores/cm^2 or larger showed power density superior to Nafion®-based systems, as depicted in Fig. 14,(b).

In most studies, PSiMs are used in the core system of the micro fuel cell. *Sabaté* et al.[32] used microfabrication techniques to create current collectors for methanol micro fuel cells. A thin layer of noble metal was electroplated onto the membranes to act as electrodes. Metal catalyst was also added to the PSiM via electrodeposition. Two current collectors were easily bound to PDMS-Nafion® membranes in order to form the final devices. *Yu et al.*[36] used a similar fabrication process for the cathode of their self-breathing hydrogen micro fuel cell. They compared the performance of the electrode to conventional catalyst coated carbon-paper: the PSi cathode possessed a stronger catalytic activity and higher catalyst consumption efficiency. Moreover, to optimise the electrodes and improve the fuel cell efficiency, a catalyst was deposited inside the porous matrix during the membrane fabrication, as the presence of uncoated PSi was found to reduce the cell performance [30]. The measured power density was in the order of magnitude of 10^2 mW/cm^2 but largely varied from one prototype to another, suggesting the need of further optimisation [98]. Another technique to incorporate a catalyst layer to porous silicon was developed by *Yang et al.*[35]: carbon nanotubes were grown onto the PSiMs, serving as catalyst support because of their large surface area and their enhanced capacity to remove CO_2. While some studies focus on the catalyst layer deposition, others concentrate on the electric conduction layer: *Starkov et al.*[33] replaced the noble metal deposited on the PSiM-based current collectors by graphene, which resulted in highly conductive electrodes.

Finally, *Yuzova et al.*[57,37] demonstrated that a multilayered PSiM can serve as a monotlithic MEA for hydrogen micro fuel cells. A mesoporous layer, serving as ion-exchange membrane, was surrounded by two macroporous layers, which served as gas diffusion layer, catalyst support and electrodes. A controlled deposition of nickel not only created a metal contact, but closed off all macroporous side pores that would induce gas-transport losses. Iridium catalyst was then deposited on the nickel layer. While the fuel cell performance remained very low, reaching a power density of 16 mW/cm^2, the potential of monolithic PSi-based MEAs was demonstrated.

6. Integration challenges

In the main applications detailed in Section 5, PSiMs are mostly used because of their permeability, which enables a flow-through operation. Less developed areas of application, such as electronics for example, use PSiMs for properties that are not strictly structural. While isolating PSi from its bulk substrate was mainly used as a characterisation tool in the early years of PSiM-based research, it has now become a new source of applications: by fabricating PSiMs, the effect of the underlying bulk silicon on the properties, more specifically on the thermal and electrical properties, is completely eliminated. This is illustrated by the emergence of thermal [24–26] and RF [61,58] devices based on PSiMs.

With the advent of these novel applications and fabrication routes, new questions are raised, the main one being how to bring PSiMs from a research environment to the industry. Recent years have seen the slow rise of commercially available PSiMs, although only in a limited range of physical features and small areas. For instance, SmartMembranes GmbH (Halle, Germany) produces macroporous PSiMs using electochemical etching, with a pore diameter ranging from 1 μm to 17.4 μm and a membrane thickness going from 15 μm to 500 μm. Simpore Inc. (Rochester, NY, USA) on the other hand produces nanoporous silicon and silicon nitride membranes, characterised by a mesoporous pore size and a nanometer-scaled thickness. A final example of commercialisation is Aquamarijn (Zutphen, the Netherlands), where macroporous silicon nitride membranes are manufactured with a thickness of 0.5 μm – 2 μm. However, these commercial porous membranes are mainly used in research environments and their relative high cost (up to 48€ for a 1 cm^2 membrane) precludes their inclusion in widely industrialised products.

Although PSiMs have a long track record for basic and applied research, their industrial applications remain severely limited by large-scale integration challenges and constraints. Nonetheless, because PSiMs are compatible with microfabrication techniques and cleanroom environment, they have the potential to become integrated in microelectronics devices. This potential is currently hampered by a series of obstacles, among which the lack of reliable processes and equipment, the low reproducibility, the need for high quality silicon substrates and the disparate properties. There are still too many unknowns in the field of PSi and PSiMs that block the transition from research to industry. The absence of standards in the PSi-research community makes it difficult to fill the present gaps of knowledge. PSiM-based research occurs sporadically and isolates itself in "low budget" fields of research and application. To fully benefit from the properties of PSi and introduce innovative PSi-based products to the market, PSiMs must be combined with

other microelectronics devices, such as integrated light sources, communications systems or electronic interfaces. This is only possible if the access to cleanrooms and microfabrication techniques is guaranteed.

Yet, when the access to Complementary metal-oxide-semiconductor (CMOS) technologies is assured, the introduction of PSiMs hinders further microfabrication process steps. The mechanical stability of the substrate is indeed compromised and some process steps such as high temperature annealing are incompatible with PSi since they cause cracking and bending. This makes the integration of PSiMs at a wafer level into a full CMOS process difficult, but not impossible. Indeed, PSi was already integrated in a CMOS process over a decade ago, namely in Bosch's Advanced Porous Silicon Membrane (APSM) process, which is used in the fabrication of pressure sensors for automotive applications [179–182]. More recent advances and challenges in the integration of PSi at the industrial level are presented by *Gautier et al.*[183]. Despite their limited reproducibility and homogeneity, the various attempts at industrialisation discussed by the authors show great promise. Two examples of prototypes worth mentioning are *Barillaro et al.*'s gas sensor [184,185] and *Capelle et al.*'s RF devices [186,187], both produced in Si processing environments and integrated with CMOS electronics. Moreover, novel work from *Scheen et al.*[58] presented a step towards large-scale industrial production. They demonstrated the integration of porous silicon in a post-process anodisation: porosification occurs as the last step of the process and only involves the backside of the wafer, leaving the front-side circuitry intact. This progress in the integration of PSi and PSiMs paves the way for the development of new application and for future industrialisation attempts.

7. Conclusion and future outlook

PSi membranes are very promising and versatile materials for many applications. In terms of fabrication, the processes are varied but are becoming more and more reliable. While the fabrication of freestanding membranes enables the reuse of the silicon substrate, self-supporting and lateral membrane are more robust and their fabrication process is more repeatable. On the other hand, microfabricated PSiMs have more controlled geometrical features. For all types of membranes, the integration possibilities are numerous. Recent research provides also a better understanding of PSiM properties: mechanical properties were found to depend of physical features; mass transport is improved compared to close-ended PSi layers; PSi's low thermal conductivity is maintained; carrier dynamics have been successfully modelled; and finally, PSiMs are biocompatible and biodegradable, unless their surface is modified. Many other properties however yet remain to be investigated.

A major part of this review focused on applications, which are numerous and varied. Three major ones emerged, namely scaffolding for cell culture, biosensing and fuel cell miniaturisation. PSiMs were observed to be excellent candidates for cell culture materials because their biocompatibility, although surface functionalisation was sometimes required to promote cell adhesion. The PSiM-based scaffolds were used to investigate cell migration behaviour or to build "organ-on-chip" device. The optical features of PSi also enabled an optical monitoring of the scaffolds. More recent work studied complex scaffold integrations, mimicking multilayered tissue architectures. Biosensing was the focal point of many new studies. Optical biosensors have mainly been researched, relying on changes in the reflection or transmission spectra to detect the targeted analyte. This trend further migrated to other optical techniques, like SERS for instance. For all detection techniques, the challenge remains the surface functionalisation, which adds the recognition element to the sensors. Furthermore, a significant part of research on PSiM-based biosensors concentrated on nanopore-based DNA sequencing, especially on the possibility to sequence DNA in parallel by optically monitoring the DNA translocation events. The third major application field concerned energy conversion. We conveyed that PSiMs comprise very promising materials for fuel cell miniaturisation, addressing many issues encountered in this research area. PSiMs could be used for fuel supply, as ion-exchange membrane, in the core system, or for a combination of several of these functions.

This review demonstrates the real interest in PSiMs for research and fundamental studies. As discussed in Section 6, the integration challenges are key and will determine the future of PSiM-based research. The main challenge to the transition from lab to fab environment is not only the need for more reliable processes and equipment that would allow high volume throughput production of PSiMs-based devices, but also the lack of standardisation. Few attempts at industrialisation of PSi have been made, as it still remains laborious to render electrochemical etching controlled, repeatable and reliable. The mechanical integrity of the PSiMs is a source of problems as well. This has partially been solved by the fabrication of lateral PSiMs, but the limited physical properties achievable for such membranes are drawbacks. Further research is needed to find easy and reliable methods to stabilise PSiMs, using pieces of equipment that enable large surface treatments. However, based on the studies reviewed here, it is reasonable to expect that PSiMs will move from research labs to commercial applications in the future.

Authors' contributions

Roselien Vercauteren: Conceptualisation, Investigation, Writing– Original draft preparation **Gilles Scheen**: Writing – Review & Editing **Jean-Pierre Raskin**: Writing – Review & Editing **Laurent A. Francis**: Conceptualisation, Writing – Review & Editing

Declaration of interests

None.

Declaration of Competing Interest

The authors report no declarations of interest.

Acknowledgments

This work was supported by the FNRS (National Fund for Scientific Research) through a FRIA (*Fonds pour la formation à la Recherche dans l'Industrie et dans l'Agriculture*) grant to R. Vercauteren.

References

[1] S. Franssila, Introduction to Microfabrication, Wiley, 2004.
[2] A. Uhlir Jr., Electrolytic shaping of germanium and silicon, Bell Syst. Tech. J 35 (1956) 333–347.
[3] L.T. Canham, Silicon quantum wire array fabrication by electrochemical and chemical dissolution of wafers, Appl. Phys. Lett. 57 (1990) 1046–1048.
[4] V. Lehmann, U. Gösele, Porous silicon formation: a quantum wire effect, Appl. Phys. Lett. 58 (1991) 856–858.
[5] D.L. Kendall, A new theory for the anisotropic etching of silicon and some underdeveloped chemical micromachining concepts, J. Vac. Sci. Tech. A 8 (1990) 3598–3605.
[6] G. Kittilsland, G. Stemme, B. Nordén, A sub-micron particle filter in silicon, Sensor. Actuat. A Phys. 23 (1990) 904–907.
[7] P. Dardano, A. Caliò, J. Politi, I. Rea, I. Rendina, L.D. Stefano, Optically monitored drug delivery patch based on porous silicon and polymer microneedles, Biomed. Opt. Express. 7 (2016) 1645–1655, Optical Society of America.
[8] J.P.S. DesOrmeaux, J.D. Winans, S.E. Wayson, T.R. Gaborski, T.S. Khire, C.C. Striemer, J.L. McGrath, Nanoporous silicon nitride membranes fabricated

from porous nanocrystalline silicon templates, Nanoscale 6 (2014) 10798–10805, The Royal Society of Chemistry.
[9] C. Drieschner, S. Könemann, P. Renaud, K. Schirmer, Fish-gut-on-chip: development of a microfluidic bioreactor to study the role of the fish intestine in vitro, Lab. Chip. 19 (2019) 3268–3276, The Royal Society of Chemistry.
[10] K. Hill, S.N. Walker, A. Salminen, H.L. Chung, X. Li, B. Ezzat, J.J. Miller, J.S. DesOrmeaux, J. Zhang, A. Hayden, T. Burgin, L. Piraino, M.N. May, T.R. Gaborski, J.A. Roussie, J. Taylor, L. DiVincenti, A.A. Shestopalov, J.L. McGrath, D.G. Johnson, Second generation nanoporous silicon nitride membranes for high toxin clearance and small format hemodialysis, Adv. Healthc. Mater 9 (2020) 1900750.
[11] Y. Hosseini, S. Soltanian-Zadeh, V. Srinivasaraghavan, M. Agah, A silicon-based porous thin membrane as a cancer cell transmigration assay, J. Microelectromech. Syst. 26 (2017) 308–316.
[12] Y.D. Irani, S. Klebe, S.J.P. McInnes, M. Jasieniak, N.H. Voelcker, K.A. Williams, oral mucosal epithelial cells grown on porous silicon membrane for transfer to the rat eye, Sci. Rep. 7 (2017) 1–11, Number: 1 Publisher: Nature Publishing Group.
[13] B.J. Nehilla, N. Nataraj, T.R. Gaborski, J.L. McGrath, Endothelial vacuolization induced by highly permeable silicon membranes, Acta. Biomater. 10 (2014) 4670–4677.
[14] Y. Pei, S.H. Shahoei, Y. Li, P.J. Reece, E.R. Nelson, J.J. Gooding, K.A. Kilian, Vertical integration of cell-laden hydrogels with bioinspired photonic crystal membranes, Adv. Mater. Interfaces 5 (2018) 1801233.
[15] T.H. Punde, W.-H. Wu, P.-C. Lien, Y.-L. Chang, P.-H. Kuo, M.D.-T. Chang, K.-Y. Lee, C.-D. Huang, H.-P. Kuo, Y.-F. Chan, P.-C. Shih, C.-H. Liu, A biologically inspired lung-on-a-chip device for the study of protein-induced lung inflammation, Integr. Biol 7 (2015) 162–169.
[16] B.N.G. Sajay, C.S. Yin, Q. Ramadan, Optimization of micro-fabricated porous membranes for intestinal epithelial cell culture and in vitro modeling of the human intestinal barrier, J. Micromech. Microeng. 27 (2017) 124004.
[17] H. So, K. Lee, Y.H. Seo, N. Murthy, A.P. Pisano, Hierarchical silicon nanospikes membrane for rapid and high-throughput mechanical cell lysis, ACS. Appl. Mater. Interfaces. 6 (2014) 6993–6997, American Chemical Society.
[18] W.Y. Tong, M.J. Sweetman, E.R. Marzouk, C. Fraser, T. Kuchel, N.H. Voelcker, Towards a subcutaneous optical biosensor based on thermally hydrocarbonised porous silicon, Biomaterials 74 (2016) 217–230.
[19] Y. Zhao, G. Gaur, S.T. Retterer, P.E. Laibinis, S.M. Weiss, Flow-through porous silicon membranes for real-time label-free biosensing, Anal. Chem. 88 (2016) 10940–10948.
[20] H.-G. Kim, K.-W. Lee, Electrostatic gas sensor with a porous silicon diaphragm, Sensor Actuat. B. Chem. 219 (2015) 10–16.
[21] N. Kumar, E. Froner, R. Guider, M. Scarpa, P. Bettotti, Investigation of non-specific signals in nanoporous flow-through and flow-over based sensors, Analyst. 139 (2014) 1345.
[22] N.P. Ratchagar, V.T. Fidal, P. Bhadra, A. Ghosh, A. Chadha, E. Bhattacharya, Sensor for continuous and real-time monitoring of biomolecule permeation through ultrathin silicon nanoporous membranes, IEEE Sens. J. 19 (2019) 4419–4427, IEEE Sensors Journal.
[23] N. Yu, J. Wu, Rapid and reagentless detection of thrombin in clinic samples via microfluidic aptasensors with multiple target-binding sites, Biosens. Bioelectron. 146 (2019) 111726.
[24] I.-T. Chen, A.D. Stroock, A tree-on-a-chip: design and analysis of MEMS-based superheated loop heat pipes exploiting nanoporous silicon membranes, J. Phys. Conf. Ser. 557 (2014) 012067.
[25] D. Hanks, J. Sircar, Z. Lu, D. Antao, K. Bagnall, B. Barabadi, T. Salamon, E. Wang, in: 2016 Solid-State, Actuators, and Microsystems Workshop Technical Digest, Transducer Research Foundation, Hilton Head, South Carolina USA, 2016, pp. 380–383.
[26] F. Lucklum, A. Schwaiger, B. Jakoby, Highly insulating, fully porous silicon substrates for high temperature micro-hotplates, Sensor. Actuat. A Phys. 213 (2014) 35–42.
[27] M.G. Bölen, T. Karacali, Crossover of ion through porous silicon based membrane, 5th International Conference on Electrical and Electronic Engineering (ICEEE) (2018) 302–305, ISSN: null.
[28] R. Haddad, J. Thery, B. Gauthier-Manuel, K. Elouarzaki, M. Holzinger, A. Le Goff, G. Gautier, J. El Mansouri, A. Martinent, S. Cosnier, High performance miniature glucose/O2 fuel cell based on porous silicon anion exchange membrane, Electrochem. Commun. 54 (2015) 10–13.
[29] G. Nagayama, A. Kuromaru, M. Kaneda, T. Tsuruta, Effects of nano/microstructures on performance of Si-based microfuel cells, Appl. Therm. Eng. 72 (2014) 298–303.
[30] I. Morisawa, T. Suzuki, N. Katayama, K. Dowaki, M. Hayase, Miniature fuel cell with monolithically fabricated Si electrodes - uniformity of catalyst layer thickness -, J. Phys. Conf. Ser. 557 (2014) 012108.
[31] A. Roland, A. Dupuy, D. Machon, F. Cunin, N. Louvain, B. Fraisse, A. Boucherif, L. Monconduit, In-depth study of annealed porous silicon: Understand the morphological properties effect on negative LiB electrode performance, Electrochim. Acta 323 (2019) 134758.
[32] N. Sabaté, J.P. Esquivel, J. Santander, J.G. Hauer, R.W. Verjulio, I. Gràcia, M. Salleras, C. Calaza, E. Figueras, C. Cané, L. Fonseca, New approach for batch microfabrication of silicon-based micro fuel cells, Microsyst. Technol. 20 (2014) 341–348.
[33] V.V. Starkov, D.M. Sedlovets, M.A. Knyazev, A.N. Red'kin, Composite electrodes for current sources based on graphene-like films in porous silicon, Prot. Met. Phys. Chem. Surf. 53 (2017) 85–87.
[34] W.J.C. Vijselaar, P. Perez-Rodriguez, P.J. Westerik, R.M. Tiggelaar, A.H.M. Smets, H. Gardeniers, J. Huskens, A stand-alone Si-based porous photoelectrochemical cell, Adv. Energy. Mater. 9 (2019) 1803548, http://dx.doi.org/10.1002/aenm.201803548, -eprint:.
[35] C.-R. Yang, C.-W. Lu, P.-C. Fu, C. Cheng, Y.-C. Chiou, R.-T. Lee, S.-F. Tseng, Performance evaluation of μDMFCs based on porous-silicon electrodes and methanol modification, Energy 192 (2020) 116666.
[36] Z. Yu, D. Zheng, K. Zhang, T. Yang, Y. Chen, X. Li, Optimally catalyzed porous-silicon electrode of self-breathing micro fuel cells, Microsyst. Technol. 23 (2017) 3257–3262.
[37] V.A. Yuzova, F.F. Merkushev, E.A. Lyaykom, Formation of cross-cutting structures with different porosity on thick silicon wafers, Mod. Electron. Mater. 3 (2017) 72–75.
[38] C. Chiappini, E. De Rosa, J.O. Martinez, X. Liu, J. Steele, M.M. Stevens, E. Tasciotti, Biodegradable silicon nanoneedles delivering nucleic acids intracellularly induce localized in vivo neovascularization, Nat. Mater. 14 (2015) 532–539, a Number: 5 Publisher: Nature Publishing Group.
[39] C. Chiappini, J.O. Martinez, E. De Rosa, C.S. Almeida, E. Tasciotti, M.M. Stevens, Correction to biodegradable nanoneedles for localized delivery of nanoparticles in vivo: exploring the biointerface, ACS Nano 9 (2015) 7730, b American Chemical Society.
[40] C. Chiappini, P. Campagnolo, C.S. Almeida, N. Abbassi-Ghadi, L.W. Chow, G.B. Hanna, M.M. Stevens, Mapping local cytosolic enzymatic activity in human esophageal mucosa with porous silicon nanoneedles, Adv. Mater. 27 (2015) 5147–5152, http://dx.doi.org/10.1002/adma.201501304, c eprint:.
[41] S. Gopal, C. Chiappini, J. Penders, V. Leonardo, H. Seong, S. Rothery, Y. Korchev, A. Shevchuk, M.M. Stevens, Porous silicon nanoneedles modulate endocytosis to deliver biological payloads, Adv. Mater. 31 (2019) 1806788, http://dx.doi.org/10.1002/adma.201806788, eprint:.
[42] E. Blanco, H. Shen, M. Ferrari, Principles of nanoparticle design for overcoming biological barriers to drug delivery, Nat. Biotechnol. 33 (2015) 941–951.
[43] R. Xu, G. Zhang, J. Mai, X. Deng, V. Segura-Ibarra, S. Wu, J. Shen, H. Liu, Z. Hu, L. Chen, Y. Huang, E. Koay, Y. Huang, J. Liu, J.E. Ensor, E. Blanco, X. Liu, M. Ferrari, H. Shen, An injectable nanoparticle generator enhances delivery of cancer therapeutics, Nat. Biotechnol. 34 (2016) 414–418, Number: 4 Publisher: Nature Publishing Group.
[44] A. Parodi, N. Quattrocchi, A.L. van de Ven, C. Chiappini, M. Evangelopoulos, J.O. Martinez, B.S. Brown, S.Z. Khaled, I.K. Yazdi, M.V. Enzo, L. Isenhart, M. Ferrari, E. Tasciotti, Synthetic nanoparticles functionalized with biomimetic leukocyte membranes possess cell-like functions, Nat. Nanotechnol. 8 (2013) 61–68, Number: 1 Publisher: Nature Publishing Group.
[45] T. Tieu, M. Alba, R. Elnathan, A. Cifuentes-Rius, N.H. Voelcker, Advances in porous silicon-based nanomaterials for diagnostic and therapeutic applications, Adv. Ther. 2 (2019) 1800095.
[46] T. Kumeria, S.J.P. McInnes, S. Maher, A. Santos, Porous silicon for drug delivery applications and theranostics: recent advances, critical review and perspectives, Expert. Opin. Drug. Del. 14 (2017) 1407–1422.
[47] H. Alhmoud, D. Brodoceanu, R. Elnathan, T. Kraus, N.H. Voelcker, A MACEing silicon: towards single-step etching of defined porous nanostructures for biomedicine, Prog. Mater. Sci. (2019) 100636.
[48] L. Canham, Handbook of Porous Silicon, Springer, New York, 2014.
[49] K.W. Kolasinski, Electron transfer during metal-assisted and stain etching of silicon, Semicond. Sci. Technol. 31 (2016) 014002.
[50] Z.C. Feng, R. Tsu, Porous Silicon, WORLD SCIENTIFIC, 1994.
[51] G. Scheen, Metal Electrode Integration And Palladium Nanoparticule Functionalization On A Miniaturized Macroporous Silicon Chemiresistor, UCL - Université Catholique de Louvain, 2015, Ph.D. thesis.
[52] M. Sailor, Porous Silicon in Practice: Preparation, Characterization and Applications, Wiley, 2012.
[53] V. Lehmann, Electrochemistry of Silicon: Instrumentation, Science, Materials and Applications, Wiley, 2002.
[54] G. Korotcenkov, Porous Silicon: From Formation to Application: Formation and Properties, Volume One: Formation and Properties, CRC Press, 2016, Google-Books-ID: JWjdCgAAQBAJ.
[55] J. Zheng, M. Christophersen, P.L. Bergstrom, Thick macroporous membranes made of p-type silicon, Phys. Status. Solidi. A 202 (2005) 1402–1406.
[56] F. Lucklum, A. Schwaiger, B. Jakoby, Development and investigation of thermal devices on fully porous silicon substrates, IEEE Sens. J. 14 (2014) 992–997, IEEE Sensors Journal.
[57] V.A. Yuzova, F.F. Merkushev, O.V. Semenova, A monolithic silicon-based membrane-electrode assembly for micro fuel cells, Tech. Phys. Lett. 43 (2017) 764–766.
[58] G. Scheen, R. Tuyaerts, M. Rack, L. Nyssens, J. Rasson, M. Nabet, J.-P. Raskin, Post-process porous silicon for 5G applications, Solid State. Electron. 168 (2020) 107719.
[59] A. Chiadò, C. Novara, A. Lamberti, F. Geobaldo, F. Giorgis, P. Rivolo, Immobilization of oligonucleotides on metal-dielectric nanostructures for miRNA detection, Anal. Chem. 88 (2016) 9554–9563, American Chemical Society.
[60] N.E. Preobrazhenskiy, E.V. Astrova, S.I. Pavlov, V.B. Voronkov, A.M. Rumyantsev, V.V. Zhdanov, Anodes for Li-ion batteries based on p-Si with self-organized macropores, Semiconductors 51 (2017) 78–87.

[61] B. Bardet, S. Desplobain, J. Billoué, L. Ventura, G. Gautier, Integration of low-loss inductors on thin porous silicon membranes, Microelectron. Eng. 194 (2018) 96–99.
[62] H. Ning, N.A. Krueger, X. Sheng, H. Keum, C. Zhang, K.D. Choquette, X. Li, S. Kim, J.A. Rogers, P.V. Braun, Transfer-Printing of Tunable Porous Silicon Microcavities with Embedded Emitters, ACS Photonics 1 (2014) 1144–1150, American Chemical Society.
[63] G.V. Li, E.V. Astrova, A.M. Rumyantsev, V.B. Voronkov, A.V. Parfen'eva, V.A. Tolmachev, T.L. Kulova, A.M. Skundin, Microstructured silicon anodes for lithium-ion batteries, Russ. J. Electrochem. 51 (2015) 899–907.
[64] R. Mentek, D. Hippo, B. Gelloz, N. Koshida, Photovoltaic effect with high open circuit voltage observed in electrochemically prepared nanocrystalline silicon membranes, Mat. Sci. Eng. B 190 (2014) 33–40.
[65] G.V. Li, E.V. Astrova, N.E. Preobrazhenskii, A.M. Rumyantsev, S.I. Pavlov, E.V. Beregulin, Negative electrodes for lithium-ion batteries obtained by photoanodization of solar-grade silicon, Tech. Phys. 64 (2019) 660–665.
[66] M. Balucani, K. Kholostov, V. Varlamava, F. Palma, M. Izzi, L. Serenelli, M. Tucci, Porous silicon solar cells, IEEE 15th International Conference on Nanotechnology (IEEE-NANO) (2015) 724–727, ISSN: null.
[67] C. Novara, A. Lamberti, A. Chiadò, A. Virga, P. Rivolo, F. Geobaldo, F. Giorgis, Surface-enhanced Raman spectroscopy on porous silicon membranes decorated with Ag nanoparticles integrated in elastomeric microfluidic chips, RSC Adv. 6 (2016) 21865–21870.
[68] C. Novara, A. Chiadò, N. Paccotti, S. Catuogno, C.L. Esposito, G. Condorelli, V. De Franciscis, F. Geobaldo, P. Rivolo, F. Giorgis, SERS-active metal-dielectric nanostructures integrated in microfluidic devices for label-free quantitative detection of miRNA, Faraday Discuss. 205 (2017) 271–289.
[69] D. Martín-Sánchez, S. Ponce-Alcántara, J. García-Rupérez, Sensitivity comparison of a self-standing porous silicon membrane under flow-through and flow-over conditions, IEEE Sens. J. 19 (2019) 3276–3281, IEEE Sensors Journal.
[70] I.S. Kryukova, D.S. Dovzhenko, Y.P. Rakovich, I.R. Nabiev, Enhancement of the photoluminescence of semiconductor nanocrystals in transfer-printed microcavities based on freestanding porous silicon photonic crystals, J. Phys. Conf. Ser. 1439 (2020) 012018.
[71] N. Reta, A. Michelmore, C. Saint, B. Prieto-Simón, N.H. Voelcker, Porous silicon membrane-modified electrodes for label-free voltammetric detection of MS2 bacteriophage, Biosens. Bioelectron. 80 (2016) 47–53.
[72] F. Morales-Morales, L. Palacios-Huerta, S.A. Cabañas-Tay, A. Coyopol, A. Morales-Sánchez, Luminescent Si quantum dots in flexible and semitransparent membranes for photon down converting material, Opt. Mater. 90 (2019) 220–226.
[73] I.-T. Chen, D.A. Sessoms, Z. Sherman, E. Choi, O. Vincent, A.D. Stroock, Stability limit of water by metastable vapor-liquid equilibrium with nanoporous silicon membranes, J. Phys. Chem. B 120 (2016) 5209–5222, American Chemical Society.
[74] M.R. Jimenéz-Vivanco, G. García, J. Carrillo, V. Agarwal, T. Díaz-Becerril, R. Doti, J. Faubert, J.E. Lugo, Porous Si-SiO 2 based UV microcavities, Sci. Rep. 10 (2020) 1–21, a Number: 1 Publisher: Nature Publishing Group.
[75] M.R. Jimenéz-Vivanco, G. García, J. Carrillo, F. Morales-Morales, A. Coyopol, M. Gracia, R. Doti, J. Faubert, J.E. Lugo, Porous Si-SiO2 UV microcavities to modulate the responsivity of a broadband photodetector, Nanomaterials 10 (2020) 222, b Number: 2 Publisher: Multidisciplinary Digital Publishing Institute.
[76] L.G. Cencha, C. Antonio Hernández, L. Forzani, R. Urteaga, R.R. Koropecki, Optical performance of hybrid porous silicon-porous alumina multilayers, J. Appl. Phys. 123 (2018) 183101.
[77] D.J.J. Fandio, S. Sauze, A. Boucherif, R. Arès, D. Morris, Structural, optical and terahertz properties of graphene-mesoporous silicon nanocomposites, Nanoscale Adv. 2 (2020) 340–346, RSC.
[78] S. De La Luz-Merino, M.E. Calixto, A. Méndez-Blas, Nanostructured CuInSe2 by electrodeposition with the assistance of porous silicon templates, Mater. Chem. Phys. 163 (2015) 362–368.
[79] Y. Zhao, G. Gaur, R.L. Mernaugh, P.E. Laibinis, S.M. Weiss, Comparative kinetic analysis of closed-ended and open-ended porous sensors, Nanoscale. Res. Lett. 11 (2016) 1.
[80] Z. Wu, X. Wang, L. Liu, A. Passive, Vapor-feed direct methanol fuel cell based on a composite pervaporation membrane, J. Microelectromech. Syst. 24 (2015) 207–215.
[81] N. Burham, A.A. Hamzah, J. Yunas, B.Y. Majlis, Electrochemically etched nanoporous silicon membrane for separation of biological molecules in mixture, J. Micromech. Microeng 27 (2017) 075021, a.
[82] N. Burham, A.A. Hamzah, B. Yeop Majlis, Self-adjusting electrochemical etching technique for producing nanoporous silicon membrane, in: New Research on Silicon - Structure, Properties, Technology, IntechOpen, 2017.
[83] M. Wang, L. Liu, X. Wang, A novel proton exchange membrane based on sulfo functionalized porous silicon for monolithic integrated micro direct methanol fuel cells, Sensor. Actuat. B. Chem. 253 (2017) 621–629.
[84] M. Wang, L. Liu, X. Wang, Effects of grafting parameters on the properties of proton exchange membranes based on sulfo-functionalized porous silicon for micro direct methanol fuel cells, J. Polym. Eng. 39 (2019) 620–627.
[85] V.V. Bolotov, K.E. Ivlev, E.V. Knyazev, I.V. Ponomareva, V.E. Roslikov, Formation of multilayer structures with integrated membranes based on porous silicon, Semiconductors 54 (2020) 609–613.
[86] T. Pichonat, B. Gauthier-Manuel, A new process for the manufacturing of reproducible mesoporous silicon membranes, J. Membr. Sci. 280 (2006) 494–500.
[87] K.H. Tantawi, B. Berdiev, R. Cerro, J.D. Williams, Porous silicon membrane for investigation of transmembrane proteins, Superlattices Microstruct. 58 (2013) 72–80.
[88] H. So, K. Lee, N. Murthy, A.P. Pisano, All-in-one nanowire-decorated multifunctional membrane for rapid cell lysis and direct DNA isolation, ACS Appl. Mater. Interfaces. 6 (2014) 20693–20699.
[89] A. Baraket, J.-P. Alcaraz, C. Gondran, G. Costa, G. Nonglaton, F. Gaillard, P. Cinquin, M.-L. Cosnier, D.K. Martin, Long duration stabilization of porous silicon membranes in physiological media: application for implantable reactors, Mater. Sci. Eng. C 108 (2020) 110359.
[90] M.A. Parashchenko, N.S. Filippov, V.V. Kirienko, S.I. Romanov, Electroosmotic pump based on asymmetric silicon microchannel membranes, Optoelectronics, Instrumentation Data Process. 50 (2014) 315–322.
[91] M.A. Parashchenko, N.S. Filippov, V.V. Kirienko, Microfluidic electric generator based on a silicon microchannel membrane, Optoelectronics, Instrumentation Data Process. 51 (2015) 94–102.
[92] V.V. Bolotov, K.E. Ivlev, E.V. Knyazev, I.V. Ponomareva, V.E. Roslikov, The formation of membranes based on oxidized two-layer porous silicon, AIP Conference Proceedings 2141, Selangor, Malaysia, p. 040017. (2019).
[93] M.S. Khan, J.D. Williams, Fabrication of solid state nanopore in thin silicon membrane using low cost multistep chemical etching, Materials 8 (2015) 7389–7400, Number: 11 Publisher: Multidisciplinary Digital Publishing Institute.
[94] M.S. Khan, N.S. Dosoky, B.K. Berdiev, J.D. Williams, Electrochemical impedance spectroscopy for black lipid membranes fused with channel protein supported on solid-state nanopore, Eur. Biophys. J. 45 (2016) 843–852.
[95] M.S. Khan, N.S. Dosoky, G. Mustafa, D. Patel, B. Berdiev, J.D. Williams, Electrophysiology of epithelial sodium channel (ENaC) embedded in supported lipid bilayer using a single nanopore chip, Langmuir 33 (2017) 13680–13688, American Chemical Society.
[96] T. Schmidt, M. Zhang, I. Sychugov, N. Roxhed, J. Linnros, Nanopore arrays in a silicon membrane for parallel single-molecule detection: fabrication, Nanotechnology 26 (2015) 314001.
[97] M. Zhang, T. Schmidt, A. Jemt, P. Sahlén, I. Sychugov, J. Lundeberg, J. Linnros, Nanopore arrays in a silicon membrane for parallel single-molecule detection: DNA translocation, Nanotechnology 26 (2015) 314002.
[98] M. Kobayashi, T. Suzuki, M. Hayase, A miniature fuel cell with monolithically fabricated Si electrodes - Reduction of residual porous Si on catalyst layer, J. Power Sources 267 (2014) 622–628.
[99] T. Leïchlé, D. Bourrier, Integration of lateral porous silicon membranes into planar microfluidics, Lab. Chip. 15 (2015) 833–838.
[100] Y. He, T. Leïchlé, Fabrication of lateral porous silicon membranes for planar microfluidics by means of ion implantation, Sensor Actuat. B. Chem. 239 (2017) 628–634.
[101] H. Hagino, S. Tanaka, N. Tanimura, K. Miyazaki, Thermal and electrical conductivities of porous Si membranes, Int. J. Thermophys. 36 (2015) 2548–2564.
[102] M. Sledzinska, B. Graczykowski, F. Alzina, U. Melia, K. Termentzidis, D. Lacroix, C.M.S. Torres, Thermal conductivity in disordered porous nanomembranes, Nanotechnology 30 (2019) 012654, IOP Publishing.
[103] A. Stephens, R. Nidetz, N. Mesyngier, M.T. Chung, Y. Song, J. Fu, K. Kurabayashi, Mass-producible microporous silicon membranes for specific leukocyte subset isolation, immunophenotyping, and personalized immunomodulatory drug screening in vitro, Lab. Chip. 19 (2019) 3065–3076.
[104] B. Graczykowski, A.E. Sachat, J.S. Reparaz, M. Sledzinska, M.R. Wagner, E. Chavez-Angel, Y. Wu, S. Volz, Y. Wu, F. Alzina, C.M.S. Torres, Thermal conductivity and air-mediated losses in periodic porous silicon membranes at high temperatures, Nat. Commun. 8 (2017) 1–9, Number: 1 Publisher: Nature Publishing Group.
[105] M. Verdier, R. Anufriev, A. Ramiere, K. Termentzidis, D. Lacroix, Thermal conductivity of phononic membranes with aligned and staggered lattices of holes at room and low temperatures, Phys. Rev. B 95 (2017) 205438, a.
[106] M. Verdier, D. Lacroix, K. Termentzidis, Heat transport in phononic-like membranes: modeling and comparison with modulated nano-wires, Int. J. Heat Mass Transfer 114 (2017) 550–558, b.
[107] T. Ghoshal, J.D. Holmes, M.A. Morris, Development of ordered, porous (Sub-25 nm Dimensions) surface membrane structures using a block copolymer approach, Sci. Rep. 8 (2018) 1–11, Number: 1 Publisher: Nature Publishing Group.
[108] S. Greil, A. Rahman, M. Liu, C.T. Black, Gas transport selectivity of ultrathin, nanoporous, inorganic membranes made from block copolymer templates, Chem. Mater. 29 (2017) 9572–9578, American Chemical Society.
[109] S.R. Gillmer, D.Z. Fang, S.E. Wayson, J.D. Winans, N. Abdolrahim, J.-P.S. DesOrmeaux, J. Getpreecharsawas, J.D. Ellis, P.M. Fauchet, J.L. McGrath, Predicting the failure of ultrathin porous membranes in bulge tests, Thin Solid Films. 631 (2017) 152–160.
[110] G.R. Madejski, K. Briggs, J.-P. DesOrmeaux, J.J. Miller, J.A. Roussie, V. Tabard-Cossa, J.L. McGrath, Monolithic fabrication of NPN/SiNx dual membrane cavity for nanopore-based dna sensing, Adv. Mater. Interfaces. 6 (2019) 1900684, http://dx.doi.org/10.1002/admi.201900684, eprint:.

[111] C. Qi, C.C. Striemer, T.R. Gaborski, J.L. McGrath, P.M. Fauchet, Highly porous silicon membranes fabricated from silicon nitride/silicon stacks, Small 10 (2014) 2946–2953.
[112] C. Zhou, N. Tambo, E.M. Ashley, Y. Liao, J. Shiomi, K. Takahashi, G.S.W. Craig, P.F. Nealey, Enhanced Reduction of Thermal Conductivity in Amorphous Silicon Nitride-Containing Phononic Crystals Fabricated Using Directed Self-Assembly of Block Copolymers, ACS Nano, American Chemical Society, 2020.
[113] M. Sairi, N. Chen-Tan, G. Neusser, C. Kranz, D.W.M. Arrigan, Electrochemical characterisation of nanoscale liquid-liquid interfaces located at focused ion beam-milled silicon nitride membranes, ChemElectroChem 2 (2015) 98–105.
[114] Y. Bdour, J. Gomez-Cruz, C. Escobedo, Structural stability of optofluidic nanostructures in flow-through operation, Micromachines 11 (2020) 373, Number: 4 Publisher: Multidisciplinary Digital Publishing Institute.
[115] R. Maboudian, Micro Devices:, Stiction and Adhesion, in: K.H.J. Buschow, R.W. Cahn, M.C. Flemings, B. Ilschner, E.J. Kramer, S. Mahajan, P. Veyssière (Eds.), Encyclopedia of Materials: Science and Technology, Elsevier, Oxford, 2001, pp. 5591–5593.
[116] T. Sumigawa, S. Ashida, S. Tanaka, K. Sanada, T. Kitamura, Fracture toughness of silicon in nanometer-scale singular stress field, Eng. Fract. Mech. 150 (2015) 161–167.
[117] G.Y. Gor, L. Bertinetti, N. Bernstein, T. Hofmann, P. Fratzl, P. Huber, Elastic response of mesoporous silicon to capillary pressures in the pores, Appl. Phys. Lett. 106 (2015) 261901.
[118] A. Grosman, J. Puibasset, E. Rolley, Adsorption-induced strain of a nanoscale silicon honeycomb, Europhys. Lett. 109 (2015) 56002.
[119] E. Rolley, N. Garroum, A. Grosman, Using capillary forces to determine the elastic properties of mesoporous materials, Phys. Rev. B 95 (2017) 064106.
[120] T. Hofmann, D. Wallacher, R. Toft-Petersen, B. Ryll, M. Reehuis, K. Habicht, Phonons in mesoporous silicon: The influence of nanostructuring on the dispersion in the Debye regime, Microporous Mesoporous Mater. 243 (2017) 263–270.
[121] X. Gong, J. Bustillo, L. Blanc, G. Gautier, FEM simulation on elastic parameters of porous silicon with different pore shapes, Int. J. Solids Struct. 190 (2020) 238–243.
[122] C. Populaire, B. Remaki, V. Lysenko, D. Barbier, H. Artmann, T. Pannek, On mechanical properties of nanostructured meso-porous silicon, Appl. Phys. Lett. 83 (2003) 1370–1372.
[123] R.S. Dariani, M. Nazari, Comparison of stress, strain, and elastic properties for porous silicon layers supported by substrate and corresponding membranes, J. Mol. Struct. 1119 (2016) 308–313.
[124] R. Guider, C. Traversa, P. Bettotti, Mechanical stress relief in porous silicon free standing membranes, Opt. Mater. Express. 5 (2015) 2128.
[125] N. Burham, A.A. Hamzah, B.Y. Majlis, Mechanical characteristics of porous silicon membrane for filtration in artificial kidney, 2014 IEEE International Conference on Semiconductor Electronics (ICSE2014) (2014) 119–122, http://dx.doi.org/10.1109/SMELEC.2014.6920810, ISSN: null.
[126] M. Fahmi bin Jaafar, R. Latif, B.Y. Majlis, Simulation on mechanical properties of porous nanocrystalline silicon membrane for artificial kidney, IEEE Regional Symposium on Micro and Nanoelectronics (RSM) (2017) 26–29, ISSN: null.
[127] R.W. Baker, Membrane Technology and Applications, John Wiley & Sons, 2012, Google-Books-ID: FhtBKUq4rL8C.
[128] R.M.A. Roque-Malherbe, Adsorption and Diffusion in Nanoporous Materials, CRC Press, 2018, Google-Books-ID: p3FQDwAAQBAJ.
[129] S. Wolf, N. Neophytou, H. Kosina, Thermal conductivity of silicon nanomeshes: effects of porosity and roughness, J. Appl. Phys. 115 (2014) 204306.
[130] J. Chen, X. Zhang, Pore-size dependence of the heat conduction in porous silicon and phonon spectral energy density analysis, Phys. Lett. A 384 (2020) 126503.
[131] Q. Liang, Y.-L. He, Q. Ren, Y.-P. Zhou, T. Xie, A detailed study on phonon transport in thin silicon membranes with phononic crystal nanostructures, Appl. Energy. 227 (2018) 731–741.
[132] R. Anufriev, J. Ordonez-Miranda, M. Nomura, Measurement of the phonon mean free path spectrum in silicon membranes at different temperatures using arrays of nanoslits, Phys. Rev. B 101 (2020) 115301.
[133] K. Valalaki, P. Benech, A. Galiouna Nassiopoulou, High seebeck coefficient of porous silicon: study of the porosity dependence, Nanoscale Res. Lett. 11 (2016) 201.
[134] G. Scheen, R. Tuyaerts, M. Rack, L. Nyssens, J. Rasson, J.-P. Raskin, Post-process local porous silicon integration method for RF application, in: 2019 IEEE MTT-S International Microwave Symposium (IMS), pp. 1291-1294. ISSN: 2576-7216.
[135] Y. Belaroussi, M. Rack, A.A. Saadi, G. Scheen, M.T. Belaroussi, M. Trabelsi, J.P. Raskin, High quality silicon-based substrates for microwave and millimeter wave passive circuits, Solid State. Electron. 135 (2017) 78–84.
[136] M. Rack, Y. Belaroussi, K. Ben Ali, G. Scheen, B. Kazemi Esfeh, J.-P. Raskin, Small-Large-Signal Performance Up To 175°C of Low-Cost Porous Silicon Substrate for RF Applications, IEEE T. Electron. Dev. 65 (2018) 1887–1895, IEEE Transactions on Electron Devices.
[137] Y. Lee, K. Lee, Sensing of dissolved-gas concentration in water using a rugate-structured porous silicon membrane, Sensor Actuat. B. Chem. 202 (2014) 417–425.
[138] M.D.R. Jiménez Vivanco, G. García, R. Doti, J. Faubert, J.E. Lugo Arce, Time-resolved spectroscopy of ethanol evaporation on free-standing porous silicon photonic microcavities, Materials 11 (2018) 894, Number: 6 Publisher: Multidisciplinary Digital Publishing Institute.
[139] W. He, I.V. Yurkevich, L.T. Canham, A. Loni, A. Kaplan, Determination of excitation profile and dielectric function spatial nonuniformity in porous silicon by using WKB approach, Opt. Express 22 (2014) 27123.
[140] J.R. Knab, X. Lu, F.A. Vallejo, G. Kumar, T.E. Murphy, L.M. Hayden, Ultrafast carrier dynamics and optical properties of nanoporous silicon at terahertz frequencies, Opt. Mater. Express 4 (2014) 300–307, Optical Society of America.
[141] A. Zakar, S.J. Park, V. Zerova, A. Kaplan, L.T. Canham, K.L. Lewis, C.D. Burgess, MWIR optical modulation using structured silicon membranes, in: K.L. Lewis, R.C. Hollins (Eds.), Proceedings Volume 9992, Emerging Imaging and Sensing Technologies, Edinburgh, United Kingdom, 2016, p. 999203, http://dx.doi.org/10.1117/12.2242287.
[142] A. Zakar, R. Wu, D. Chekulaev, V. Zerova, W. He, L. Canham, A. Kaplan, Carrier dynamics and surface vibration-assisted Auger recombination in porous silicon, Phys. Rev. B 97 (2018) 155203.
[143] W. He, R. Wu, I.V. Yurkevich, L.T. Canham, A. Kaplan, Reconstructing charge-carrier dynamics in porous silicon membranes from time-resolved interferometric measurements, Sci. Rep. 8 (2018) 1–7, Number: 1 Publisher: Nature Publishing Group.
[144] S.J. Park, A. Zakar, V.L. Zerova, D. Chekulaev, L.T. Canham, A. Kaplan, All-optical modulation in mid-wavelength infrared using porous Si membranes, Sci. Rep. 6 (2016) 1–8, Number: 1 Publisher: Nature Publishing Group.
[145] S. Anderson, H. Elliott, D. Wallis, L. Canham, J. Powell, Dissolution of different forms of partially porous silicon wafers under simulated physiological conditions, Phys. Status Solidi A Appl. Res. 197 (2003) 331–335, Cited By 186.
[146] M. Hecini, A. Khelifa, B. Bouzid, N. Drouiche, S. Aoudj, H. Hamitouche, Study of formation, stabilization and properties of porous silicon and porous silica, J. Phys. Chem. Solids 74 (2013) 1227–1234.
[147] M. Stewart, E. Robins, T. Geders, M. Allen, H. Choi, J. Buriak, Three methods for stabilization and functionalization of porous silicon surfaces via hydrosilylation and electrografting reactions, Phys. Status Solidi A Appl. Res. 182 (2000) 109–115, Cited By 57.
[148] J. Rasson, L.A. Francis, Improved Stability of Porous Silicon in Aqueous Media via Atomic Layer Deposition of Oxides, J. Phys. Chem. C 122 (2018) 331–338.
[149] J. Salonen, M. Björkqvist, E. Laine, L. Niinistö, Stabilization of porous silicon surface by thermal decomposition of acetylene, Appl. Surf. Sci. 225 (2004) 389–394.
[150] P. Bhadra, S. Sengupta, N.P. Ratchagar, B. Achar, A. Chadha, E. Bhattacharya, Selective transportation of charged ZnO nanoparticles and microorganism dialysis through silicon nanoporous membranes, J. Membr. Sci. 503 (2016) 16–24.
[151] Y. He, D. Bourrier, E. Imbernon, A. Bhaswara, X. Dollat, F. Cristiano, T. Leïchlé, Lateral porous silicon membranes with tunable pore size for on-chip separation, IEEE 29th International Conference on Micro Electro Mechanical Systems (MEMS) (2016) 497–500, ISSN: null.
[152] Y. He, D. Bourrier, E. Imbernon, T. Leïchlé, Lateral porous silicon membranes with size and charge selectivity, 2017 IEEE 12th International Conference on Nano/Micro Engineered and Molecular Systems (NEMS) (2017) 770–773, ISSN: 2474-3755.
[153] Y. He, D.S.D. Vasconcellos, V. Bardinal, D. Bourrier, E. Imbernon, L. Salvagnac, A. Laborde, X. Dollat, T. Leichlé, Lateral porous silicon interferometric transducer for sensing applications, IEEE Sens. (2018) 1–3.
[154] J.W. Kuhlmann, I.P. Mey, C. Steinem, Modulating the lateral tension of solvent-free pore-spanning membranes, Langmuir 30 (2014) 8186–8192, American Chemical Society.
[155] M. Gleisner, I. Mey, M. Barbot, C. Dreker, M. Meinecke, C. Steinem, Driving a planar model system into the 3 rd dimension: generation and control of curved pore-spanning membrane arrays, Soft Matter 10 (2014) 6228–6236, Royal Society of Chemistry.
[156] I. Kusters, A.M. van Oijen, A.J.M. Driessen, Membrane-on-a-chip: microstructured silicon/silicon-dioxide chips for high-throughput screening of membrane transport and viral membrane fusion, ACS Nano 8 (2014) 3380–3392, American Chemical Society.
[157] L.L.G. Schwenen, R. Hubrich, D. Milovanovic, B. Geil, J. Yang, A. Kros, R. Jahn, C. Steinem, Resolving single membrane fusion events on planar pore-spanning membranes, Sci. Rep. 5 (2015) 1–15, Number: 1 Publisher: Nature Publishing Group.
[158] J.W. Kuhlmann, M. Junius, U. Diederichsen, C. Steinem, SNARE-mediated single-vesicle fusion events with supported and freestanding lipid membranes, Biophys. J. 112 (2017) 2348–2356.
[159] J. Sibold, V.E. Tewaag, T. Vagedes, I. Mey, C. Steinem, Phase separation in pore-spanning membranes induced by differences in surface adhesion, Phys. Chem. Chem. Phys. (2020), 10.1039.D0CP00335B.
[160] Y. Sun, X. Zang, Y. Sun, L. Wang, Z. Gao, Lipid membranes supported by planar porous substrates, Chem. Phys. Lipids 228 (2020) 104893.
[161] W.-H. Wu, T.H. Punde, P.-C. Shih, C.-Y. Fu, T.-P. Wang, L. Hsu, H.-Y. Chang, C.-H. Liu, A capillary-endothelium-mimetic microfluidic chip for the study of immune responses, Sensor. Actuat. B. Chem. 209 (2015) 470–477.

[162] D. Martín-Sánchez, T. Angelova, J. García-Rupérez, Simultaneous refractive index sensing using an array of suspended porous silicon membranes, IEEE Sens. J. (2020) 1, IEEE Sensors Journal.
[163] N. Reta, A. Michelmore, C.P. Saint, B. Prieto-Simon, N.H. Voelcker, Label-free bacterial toxin detection in water supplies using porous silicon nanochannel sensors, ACS Sensors 4 (2019) 1515–1523, American Chemical Society.
[164] S.-W. Seo, H.R. Azmand, A.N. Enemuo, Hollow core waveguide sensor array based on a macroporous silicon membrane structure, J. Light. Technol. 37 (2019) 2036–2041, Journal of Lightwave Technology.
[165] H. Yamazaki, S. Kimura, M. Tsukahara, K. Esashika, T. Saiki, Optical detection of DNA translocation through silicon nanopore by ultraviolet light, Appl. Phys. A 115 (2014) 53–56.
[166] H. Yamazaki, S. Ito, K. Esashika, Y. Taguchi, T. Saiki, Optical observation of DNA translocation through Al2O3 sputtered silicon nanopores in porous membrane, Appl. Phys. A 122 (2016) 216.
[167] H. Yamazaki, K. Esashika, T. Saiki, A 150 nm ultraviolet excitation volume on a porous silicon membrane for direct optical observation of DNA coil relaxation during capture into nanopores, Nano Futures 1 (2017) 011001.
[168] Y. Zhao, G.A. Rodriguez, Y.M. Graham, T. Cao, G. Gaur, S.M. Weiss, Resonant photonic structures in porous silicon for biosensing, in: frontiers in biological detection: from Nanosensors to Systems IX, Int. Soc. Opt Photon. 10081 (2017) 100810D.
[169] G. Gautier, S. Kouassi, Integration of porous silicon in microfuel cells: a review, Int. J. Energy Res. 39 (2015) 1–25, http://dx.doi.org/10.1002/er.3206, eprint:.
[170] M. Ge, X. Fang, J. Rong, C. Zhou, Review of porous silicon preparation and its application for lithium-ion battery anodes, Nanotechnology 24 (2013) 422001.
[171] E. Luais, F. Ghamouss, J. Sakai, T. Defforge, G. Gautier, F. Tran-Van, Improved cycling performances of binder-free macroporous silicon Li-ion negative electrodes using room temperature ionic liquid electrolyte, J. Solid State Electrochem. 23 (2019) 937–941.
[172] N. Massad-Ivanir, E. Segal, Porous silicon for bacteria detection, in: Porous Silicon for Biomedical Applications, Elsevier, 2014, pp. 286–303.
[173] F.A. Harraz, Porous silicon chemical sensors and biosensors: a review, Sensor Actuat. B. Chem. 202 (2014) 897–912.
[174] S.N.A. Jenie, S.E. Plush, N.H. Voelcker, Recent advances on luminescent enhancement-based porous silicon biosensors, Pharm. Res. 33 (2016) 2314–2336.
[175] S. Arshavsky-Graham, N. Massad-Ivanir, E. Segal, S. Weiss, Porous silicon-based photonic biosensors: current status and emerging applications, Anal. Chem. 91 (2019) 441–467.
[176] C. RoyChaudhuri, A review on porous silicon based electrochemical biosensors: beyond surface area enhancement factor, Sensor Actuat. B. Chem. 210 (2015) 310–323.
[177] S. Mariani, L.M. Strambini, G. Barillaro, Femtomole detection of proteins using a label-free nanostructured porous silicon interferometer for perspective ultrasensitive biosensing, Anal. Chem. 88 (2016) 8502–8509.
[178] S. Ito, H. Yamazaki, M. Tsukahara, K. Esashika, T. Saiki, Salt dependence of DNA translocation dynamics through silicon nanopores detected by ultraviolet excitation, Appl. Phys. A 122 (2016) 342.
[179] S. Armbruster, F. Schafer, G. Lammel, H. Artmann, C. Schelling, H. Benzel, S. Finkbeiner, F. Larmer, R. Ruther, O. Paul, A novel micromachining process for the fabrication of monocrystalline Si-membranes using porous silicon, TRANSDUCERS '03. 12th International Conference on Solid-State Sensors, Actuators and Microsystems. Digest of Technical Papers (Cat. No.03TH8664), volume 1 (2003) 246–249, http://dx.doi.org/10.1109/SENSOR.2003.1215299.
[180] H. Artmann, F. Schaefer, G. Lammel, S. Armbruster, H. Benzel, C. Schelling, H. Weber, H.-G. Vossenberg, R. Gampp, J. Muchow, F. Laermer, S. Finkbeiner, Monocrystalline Si membranes for pressure sensors fabricated by a novel surface-micromachining process using porous silicon, MEMS Components and Applications for Industry, Automobiles, Aerospace, and Communication II, volume 4981, International Society for Optics and Photonics (2003) 65–70, http://dx.doi.org/10.1117/12.479564.
[181] K. Knese, S. Armbruster, H. Weber, M. Fischer, H. Benzel, M. Metz, H. Seidel, Novel technology for capacitive pressure sensors with monocrystalline silicon membranes, 2009 IEEE 22nd International Conference on Micro Electro Mechanical Systems (2009) 697–700, http://dx.doi.org/10.1109/MEMSYS.2009.4805478, ISSN: 1084-6999.
[182] A.C. Fischer, F. Forsberg, M. Lapisa, S.J. Bleiker, G. Stemme, N. Roxhed, F. Niklaus, Integrating MEMS and ICs, Microsyst. Nanoeng. 1 (2015) 1–16, Number: 1 Publisher: Nature Publishing Group.
[183] G. Gautier, T. Defforge, S. Desplobain, J. Billoue, M. Capelle, P. Poveda, K. Vanga, B. Lu, B. Bardet, J. Lascaud, C. Seck, A. Fevre, S. Menard, L. Ventura, Porous silicon in microelectronics: from academic studies to industry, ECS Trans. 69 (2015) 123–134.
[184] G. Barillaro, L.M. Strambini, An integrated CMOS sensing chip for NO2 detection, Sensor Actuat. B. Chem. 134 (2008) 585–590.
[185] G. Barillaro, P. Bruschi, G.M. Lazzerini, L.M. Strambini, Validation of the compatibility between a porous silicon-based gas sensor technology and standard microelectronic process, IEEE Sens. J. 10 (2010) 893–899, IEEE Sensors Journal.
[186] M. Capelle, J. Billoué, P. Poveda, G. Gautier, Porous silicon/silicon hybrid substrate applied to the monolithic integration of common-mode and bandpass rf filters, IEEE T. Electron. Dev. 62 (2015) 4169–4173.
[187] M. Capelle, J. Billoue, J. Concord, P. Poveda, G. Gautier, Monolithic integration of low-pass filters with ESD protections on p+ silicon/porous silicon substrates, Solid State Electron. 116 (2016) 12–14.

Biographies

R. Vercauteren is a PhD student at the Electrical Engineering Dpt. of the UCLouvain (Belgium) under the supervision of Prof. L. A. Francis. Her PhD thesis concerns the development of a PSi membrane for the fast detection of bacteria through their lysate. She was trained in the field of PSi by Michael Sailor during a 2-month stay inside his lab.

G. Scheen, PhD, has nearly 10 years of experience in the field of PSi and now concentrates, together with Prof. Raskin and the company Incize, on the use of PSi for radio frequency (RF) applications.

Prof. JP. Raskin, while fairly new to PSi research, is an expert in silicon nanotechnologies. His research interests are the modelling, the wideband characterization and the fabrication of advanced SOI MOSFETs as well as the micro and nanofabrication of MEMS / NEMS sensors and actuators, including the extraction of intrinsic material properties at nanometer scale.

Prof. L. A. Francis' field of expertise also relates to silicon technology, more specifically to co-integrated CMOS MEMS and NEMS sensors, harsh environment ultra-low power sensors, biomedical sensors, atomic layer deposition, bio-inspired approaches and device packaging. Over the years, he has supervised multiple PhD thesis's related to PSi and its many applications, going from sensors to energy harvesting.